nature cell biology

LETTERS

Mitochondrial outer-membrane protein FUNDC1 mediates hypoxia-induced mitophagy in mammalian cells

Lei Liu[1,2,7], Du Feng[3,7], Guo Chen[3,7], Ming Chen[1,2], Qiaoxia Zheng[1,2], Pingping Song[3], Qi Ma[1,2], Chongzhuo Zhu[1,2], Rui Wang[1], Wanjun Qi[3], Lei Huang[4,5], Peng Xue[6], Baowei Li[1,2], Xiaohui Wang[1], Haijing Jin[1], Jun Wang[1], Fuquan Yang[6], Pingsheng Liu[2], Yushan Zhu[3], Senfang Sui[4] and Quan Chen[1,2,3,8]

Accumulating evidence has shown that dysfunctional mitochondria can be selectively removed by mitophagy. Dysregulation of mitophagy is implicated in the development of neurodegenerative disease and metabolic disorders. How individual mitochondria are recognized for removal and how this process is regulated remain poorly understood. Here we report that FUNDC1, an integral mitochondrial outer-membrane protein, is a receptor for hypoxia-induced mitophagy. FUNDC1 interacted with LC3 through its typical LC3-binding motif Y(18)xxL(21), and mutation of the LC3-interaction region impaired its interaction with LC3 and the subsequent induction of mitophagy. Knockdown of endogenous FUNDC1 significantly prevented hypoxia-induced mitophagy, which could be reversed by the expression of wild-type FUNDC1, but not LC3-interaction-deficient FUNDC1 mutants. Mechanistic studies further revealed that hypoxia induced dephosphorylation of FUNDC1 and enhanced its interaction with LC3 for selective mitophagy. Our findings thus offer insights into mitochondrial quality control in mammalian cells.

Dysregulated mitochondrial activity results in either programmed cell death or the gross production of reactive oxygen species as an inevitable by-product, which causes damage to cellular DNA and proteins[1]. Thus, mitochondrial quality control is essential for normal cellular functions and is causally related to neurodegenerative and other metabolic diseases[2,3]. Recent studies have suggested that damaged mitochondria can be removed by autophagy[4]. Autophagy is a highly conserved and genetically programmed process for removing aggregated proteins and unwanted organelles[5–7]. During this process, an isolation membrane encircles a portion of the to-be-disposed contents, including damaged mitochondria, to form a double-membrane vesicle known as an autophagosome, which delivers the contents to the lysosome for bulk degradation and recycling as nutrients[6]. Several mechanisms have been proposed to account for the selective removal of dysfunctional mitochondria by autophagy[4,8,9]. Early studies have suggested that the loss of the mitochondrial membrane potential is a signal for mitophagy[8,10]. Recently, it has been revealed that endogenously or ectopically expressed parkin could be recruited towards the depolarized mitochondria through interaction with PINK1 (refs 4,11,12). Parkin, as an E3 ligase, could ubiquitinate mitochondrial surface proteins to recruit p62 or other molecules that interact with light chain 3 (LC3) for autophagosome formation[13]. This selective mitophagy could be important because mutations of parkin impair mitochondrial quality control, leading to Parkinson's disease[14]. Moreover, elimination of mitochondria by autophagy in a Nix (also known as BNIP3L)-dependent manner is critical for erythroid maturation[15,16].

Atg8, or LC3 in mammals, plays critical roles in both autophagosome membrane biogenesis and target recognition[17,18]. On autophagic stimuli, LC3-I is converted into a phosphatidylethanolamine-conjugated LC3-II form[18]. Atg32 functions as a receptor for mitophagy in yeast to regulate mitophagy through its interaction with Atg8 and Atg11 (refs 19,20). Although no orthologue of this important regulator has been found in higher-eukaryotic cells, these studies highlight the importance of mitochondrial outer-membrane proteins as a receptor to cross-talk with the autophagic machinery for selective mitophagy.

The human FUNDC1 protein contains 155 amino acids and is highly conserved from *Drosophila* to human (Supplementary Fig. S1a). Fractionation assay and immunostaining with specific antibodies against FUNDC1 clearly showed that endogenous FUNDC1 was exclusively localized on mitochondria (Fig. 1a,b). Structural and functional analyses predict that three α-helical stretches of FUNDC1 with high hydrophobicity are putative transmembrane domains

[1]The State Key Laboratory of Biomembrane and Membrane Biotechnology, Institute of Zoology, Chinese Academy of Sciences, Beijing 100101, China. [2]Graduate School of the Chinese Academy of Sciences, Beijing 100101, China. [3]College of Life Sciences, Nankai University, Tianjin 300071, China. [4]College of Life Sciences, Tsinghua University, Beijing 100084, China. [5]Center of Biomedical Analysis, Tsinghua University, Beijing 100084, China. [6]Institute of Biophysics, Chinese Academy of Sciences, Beijing 100101, China. [7]These authors contributed equally to this work.
[8]Correspondence should be addressed to Q.C. (e-mail: chenq@ioz.ac.cn)

Received 7 October 2011; accepted 14 December 2011; published online 22 January 2012; DOI: 10.1038/ncb2422

(Supplementary Fig. S1b). Clearly, the outer mitochondrial protein has its amino terminus exposed to the cytosol and carboxy terminus stretched in the intermembrane space (Supplementary Fig. S1c,d) as revealed by truncation analysis and proteinase K digestion.

In an effort to identify the potential functions of the mitochondrial outer-membrane protein, we were surprised to find that ectopically expressed FUNDC1 induced a significant increase of green fluorescent protein (GFP)–LC3 puncta, which are in close association with fragmented mitochondria (Fig. 1c). When compared with the normal mitochondrial reticulum in the vector-expressing cells, approximately 90% of the cells showed considerable GFP–LC3 punctum formation following the FUNDC1 expression. We were thus interested in understanding if and how the mitochondrial outer-membrane protein causes mitochondrial autophagy. As shown in Fig. 1d, an accumulation of the sequestered mitochondria could be clearly observed as marked by anti-VDAC1 immunogold (10 nm) within the double-membraned autophagic vesicles in the cells transfected with plasmids expressing FUNDC1–Myc under the electron microscope. The autophagic vesicle was completely absent from the cells transfected with empty vector. A three-dimensional imaging study revealed that, as shown in Fig. 1e, fragmented mitochondria were enclosed in GFP–LC3- and LAMP1-positive autolysosomes. Interestingly, FUNDC1 induced a decrease of overall mitochondrial proteins (TOM20 and VDAC1 for outer membrane, TIM23 for inner membrane) without affecting the content of other organelle markers (Fig. 1f). The decrease of mitochondrial proteins induced by FUNDC1 could be prevented by bafilomycin A1 (Fig. 1g), an inhibitor of lysosomal ATPase responsible for the acidification of lysosomes. As bafilomycin A1 was able to enhance the level of LC3-II, FUNDC1 may induce the increase of autophagic flux[21] (Fig. 1g). We also quantitatively measured the total mitochondrial volume within the cells by a commonly used three-dimensional imaging technique followed by analysis with ImageJ software. As expected, the total mitochondrial volume was significantly reduced after the expression of FUNDC1 (Fig. 1h). Furthermore, FUNDC1 was able to induce mitochondrial autophagy in both MCF7 cells and mouse embryo fibroblasts freshly isolated from mice (Supplementary Fig. S2). Taken together, our data indicate that FUNDC1 mediates mitochondrial autophagy, an important mechanism for the mitochondrial quality control.

Given the significant contribution of FUNDC1 to mitochondrial autophagy, we carried out co-immunoprecipitation to examine if FUNDC1 directly interacts with LC3, a molecule critical for autophagosome formation. As shown in Fig. 2, FUNDC1 did indeed physically interact with LC3B (Fig. 2a–d) and other LC3 homologues (Fig. 2e). Purified glutathione *S*-transferase (GST)–LC3B could pull down both bacterially expressed FUNDC1 and endogenous FUNDC1 from HeLa cell lysates, whereas ectopically expressed GFP–LC3B in HeLa cells strongly interacted with endogenous FUNDC1.

Next, we attempted to understand the molecular mechanism by which FUNDC1 mediates mitophagy. It is well known that the autophagy receptors such as p62 and Atg32 bind to LC3 and its homologues through a typical linear motif with a core consensus sequence of W/YxxL/I as previously reported[22,23] (Fig. 2f). Interestingly, we found that FUNDC1 contains a motif of Y(18)xxL(21), a characteristic LC3-interaction region (LIR), at the N-terminal region, which is exposed to cytosol. To demonstrate whether FUNDC1 interacts with LC3 through the LIR, we generated a series of mutations such as Y18A, L21A, Y18A/L21A double mutant and a deletion mutant from amino acids 18 to 21. Overexpressing these mutants in HeLa cells, followed by pulldown assays, showed that altering the sequence only at the LIR, not at other regions such as positions W32 and 33, remarkably impaired their interactions with LC3 and deletion of the entire LIR completely disrupted the event, indicating that the interaction between FUNDC1 and LC3 is through the LIR region (Fig. 2g). Collectively, these data demonstrate that FUNDC1 is an outer-mitochondrial-membrane protein that interacts with LC3 through its LIR at the cytosol-exposed N terminal (Fig. 2h). We then addressed the critical question of whether the interaction between FUNDC1 and LC3 is of functional importance for mitophagy. As expected, we have found that FUNDC1-induced mitophagy is highly dependent on its interaction with LC3. Point mutations in the LIR motif of FUNDC1 significantly impaired its induction of mitophagy, and deletion of the entire LIR completely abolished its ability to induce mitophagy in both wild-type HeLa cells (our unpublished observations) and the cells in which FUNDC1 was stably knocked down (Fig. 2i–k). The mutants also induced mitochondrial fragmentation similar to that of wild type (Fig. 3a,b). FUNDC1-induced mitophagy is dependent on ATG5, because knockdown of *ATG5* in HeLa cells completely blocked the formation of GFP–LC3 puncta, the conversion of LC3-I to LC3-II and the decrease of TIM23, which is induced by FUNDC1 (Fig. 3c,d). However, knockdown of *BECN1* did not prevent FUNDC1-induced mitophagy (Fig. 3e,f), although our previous studies showed that knockdown of *BECN1* inhibited rapamycin and starvation-induced autophagy[24–26]. Taken together, these data indicate that FUNDC1 mediates selective mitophagy by interacting with LC3 through the LIR to couple with the core autophagic machinery.

We next aimed to understand the biological significance of endogenous FUNDC1 in mitophagy. Hypoxia can induce a marked increase of GFP–LC3 punctum formation and extensive fragmentation of mitochondria, as previously reported[27,28]. Biochemical analysis showed that levels of the mitochondrial protein TIM23 and cytochrome *c* were decreased in a time-dependent manner in hypoxia treatments, whereas the endoplasmic reticulum protein calnexin was not affected (Fig. 4a). Hypoxia-induced degradation of the mitochondrial proteins such as TIM23, TOM20 and FUNDC1 could be inhibited by bafilomycin A1 (Fig. 4b). GFP–LC3 (10 nm immunogold)-positive double-membrane autophagosomes containing mitochondria marked by VDAC1 (5 nm immunogold) could be clearly observed by electron microscopy analysis as shown in Fig. 4c. Most importantly, the degradation of mitochondrial proteins could be remarkably prevented by knockdown of *FUNDC1* as revealed by western blotting analysis (Fig. 4d). In addition, the engulfment of mitochondria by autophagosomes and the loss of mitochondrial volume were not observed in *FUNDC1*-knockdown cells (Fig. 4e,f), further confirming the role of FUNDC1 in mitophagy. To further demonstrate that FUNDC1 is a specific regulator of hypoxia-induced mitophagy, we carried out rescue experiments in the cells in which *FUNDC1* is stably knocked down by a specific short hairpin RNA. Hypoxia was able to induce both the conversion of LC3-II and the reduction of TIM23 and TOM20 in the cells expressing scrambled short hairpin RNA; however, only LC3-II conversion occurred in the cells with the *FUNDC1* knockdown. As expected, wild-type FUNDC1, but not its mutants, could restore the reduction of TIM23 and

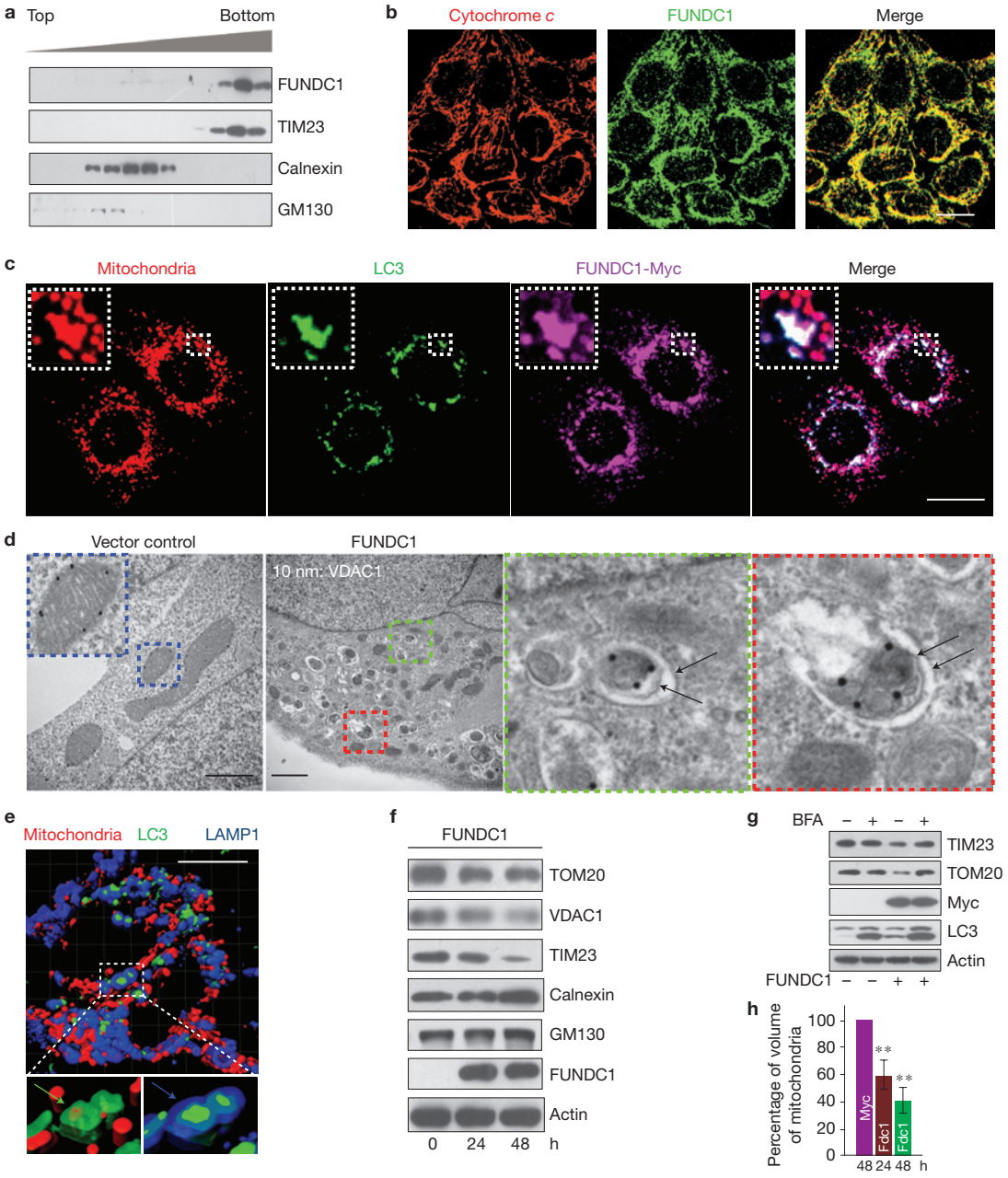

Figure 1 Mitochondrial outer-membrane protein FUNDC1 induces mitochondrial autophagy. (**a**) HeLa cells were homogenized and fractionated, followed by Percoll gradient centrifugation. Gradient fractions were analysed by western blotting with FUNDC1 and different organelle markers such as mitochondrial protein (TIM23), endoplasmic reticulum protein (calnexin) and Golgi protein (GM130). (**b**) Cells were fixed and then immunostained by FUNDC1 antibody (green) with counterstaining of mitochondrial protein cytochrome *c* (red). Scale bar, 10 μm. (**c**) GFP–LC3 (green) stable HeLa cells were transfected with plasmids encoding FUNDC1–Myc and Mito-dsRed for 24 h. The cells were then fixed and immunostained with FUNDC1 (purple, anti-Myc). Scale bar, 10 μm. (**d**) HeLa cells were co-transfected with plasmids encoding FUNDC1–Myc and GFP at a ratio of 4:1 or Myc and GFP control vector. FUNDC1–Myc-positive cells and vector control cells (both are GFP positive) were sorted and processed for immunogold electron microscopy with anti-VDAC1 antibodies (10 nm gold particles). The blue box (inset) indicates a VDAC1-positive mitochondrion. Green and red boxes indicate the autophagosomes engulfing mitochondria. Black arrows show double-membraned autophagosomes. Scale bars, 500 nm. (**e**) HeLa cells were transfected for 24 h with plasmids encoding FUNDC1–Myc, GFP–LC3, Mito-dsRed and cyan fluorescent protein–LAMP1. Live-cell Z-Stack images were collected and a representative three-dimensional reconstruction example is shown. Green and blue arrows indicate that a fragmented mitochondrion was enclosed by an LC3- and LAMP1-positive autolysosome. Scale bar, 10 μm. (**f**) HeLa cells were transfected with plasmids encoding FUNDC1–Myc for the indicated times and the mitochondrial (TIM23, TOM20, VDAC1), endoplasmic reticulum (calnexin) and Golgi marker (GM130) proteins were detected by western blotting. (**g**) HeLa cells were transfected with vector or plasmids encoding FUNDC1–Myc for 12 h in the presence or absence of bafilomycin A1 (BFA), and then TIM23, TOM20 or LC3 was detected by western blotting. (**h**) Mito-Cherry stable HeLa cells were co-transfected for 24 h or 48 h with plasmids encoding FUNDC1–Myc (Fdc1) and GFP at a ratio of 4:1 or for 48 h with Myc control vector. Five randomly picked regions of each sample were captured by confocal *z*-axis scanning and the total area of GFP positive cells and volume of mitochondria were calculated and quantified (mean ± s.e.m.; $n = 90$ cells from three independent experiments); $^{**}P < 0.01$. Uncropped images of blots are shown in Supplementary Fig. S6.

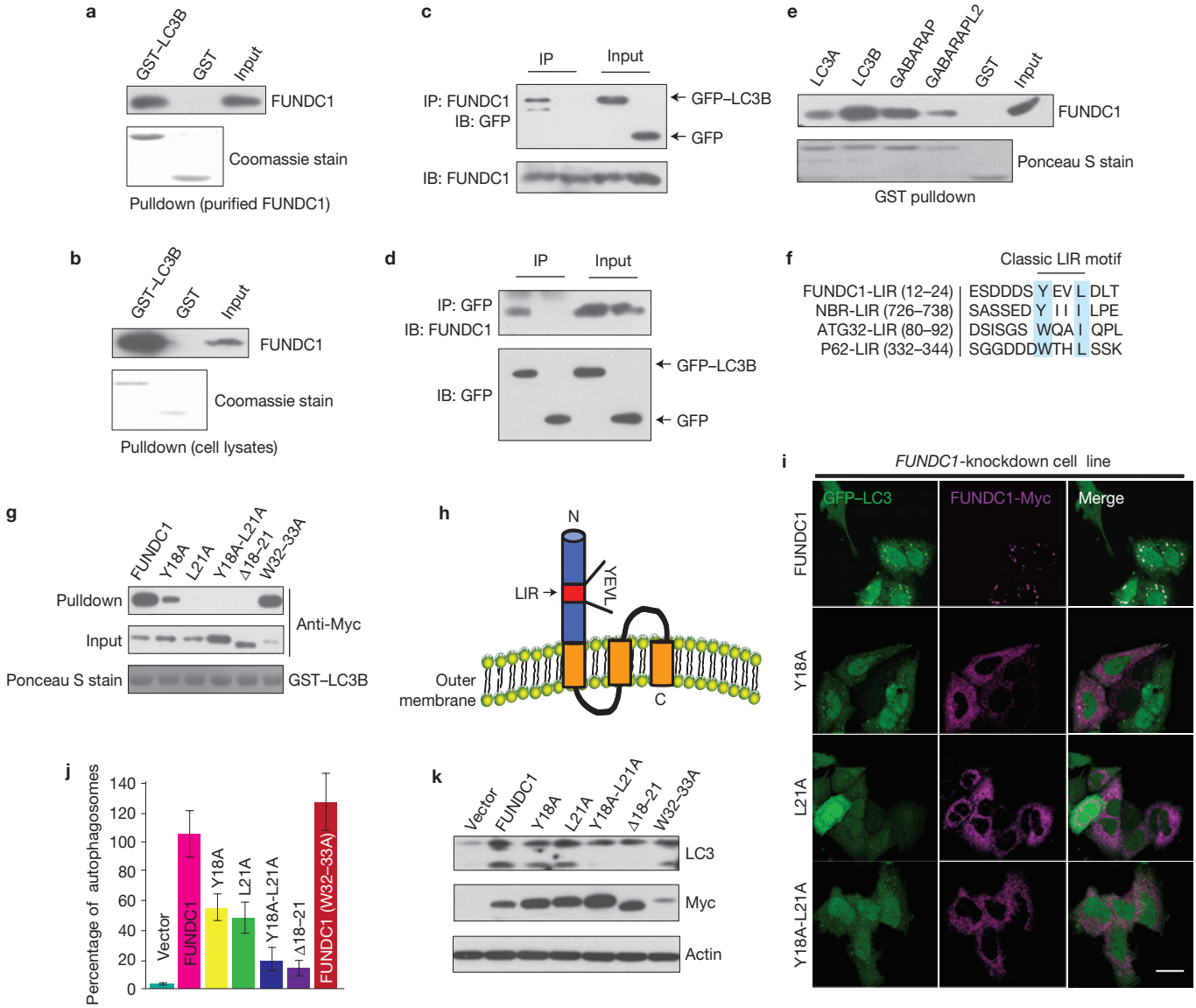

Figure 2 FUNDC1 as an LIR-motif-containing protein is a receptor for selective mitophagy. (**a**,**b**) Purified FUNDC1 protein from bacteria (**a**) or HeLa cell lysates (**b**) was incubated with immobilized GST or GST–LC3B beads and FUNDC1 was then detected with FUNDC1 antibody. Coomassie staining was used to visualize GST and GST–LC3B proteins. (**c**,**d**) HeLa cells were transfected with GFP or GFP–LC3B. 24 h after transfection, cells were collected for immunoprecipitation (IP) with anti-GFP or anti-FUNDC1 and analysed with FUNDC1 or GFP antibodies, respectively. IB, immunoblot. (**e**) FUNDC1 interacts with the LC3-family proteins. Cell extracts from HeLa cells were incubated with immobilized GST or the indicated GST fusion proteins. Immunoprecipitated FUNDC1 was detected with FUNDC1 antibody. Ponceau S staining was used to visualize GST and GST-fusion proteins. (**f**) Typical LIR sequences were aligned manually alongside FUNDC1 for comparison. The shaded regions indicate highly conserved residues in the putative LIR of FUNDC1. (**g**) HeLa cells were transfected with plasmids encoding FUNDC1–Myc or the indicated mutants. 24 h after transfection, cells were lysed and incubated with immobilized GST–LC3B. The co-precipitated proteins were detected by western blotting with Myc antibodies. Ponceau S staining was used to visualize GST-fusion proteins. (**h**) Schematic representation of FUNDC1 protein in the mitochondrial outer membrane showing the LIR at Y18evL21. (**i**) *FUNDC1*-knockdown HeLa cells were co-transfected with plasmids encoding FUNDC1–Myc or the indicated mutants (purple, anti-Myc) and GFP–LC3 for 24 h. The LIR mutants of FUNDC1 have impaired ability to induce an increase in the number of GFP–LC3 dots when compared with wild-type FUNDC1. Scale bar, 10 μm. (**j**) The number of GFP–LC3 dots in cells transfected with Myc vector or plasmids encoding wild-type or LIR-mutant FUNDC1 were quantified with ImageJ (mean ± s.e.m.; $n = 90$ cells from three independent experiments). (**k**) Western blotting to detect the changes of LC3-II induced by Myc vector and wild-type and LIR-mutant FUNDC1. Uncropped images of blots are shown in Supplementary Fig. S6.

TOM20 in *FUNDC1*-knockdown cells (Fig. 4g), despite a minor effect on the conversion of LC3-II under the hypoxic conditions. Notably, knockdown of *FUNDC1* results in significant protection of mitochondrial integrity (Fig. 4h) without affecting general autophagy as indicated by the conversion of LC3-II and the total number of GFP–LC3 puncta in hypoxia-treated cells (Fig. 4d,i). Knockdown of *FUNDC1* has no effect on starvation-induced LC3 conversion or the reduction of TIM23 and TOM20 proteins (Supplementary Fig. S3a–c), but only partially prevented mitophagy induced by the uncoupler FCCP without affecting mitochondrial fragmentation or general autophagy

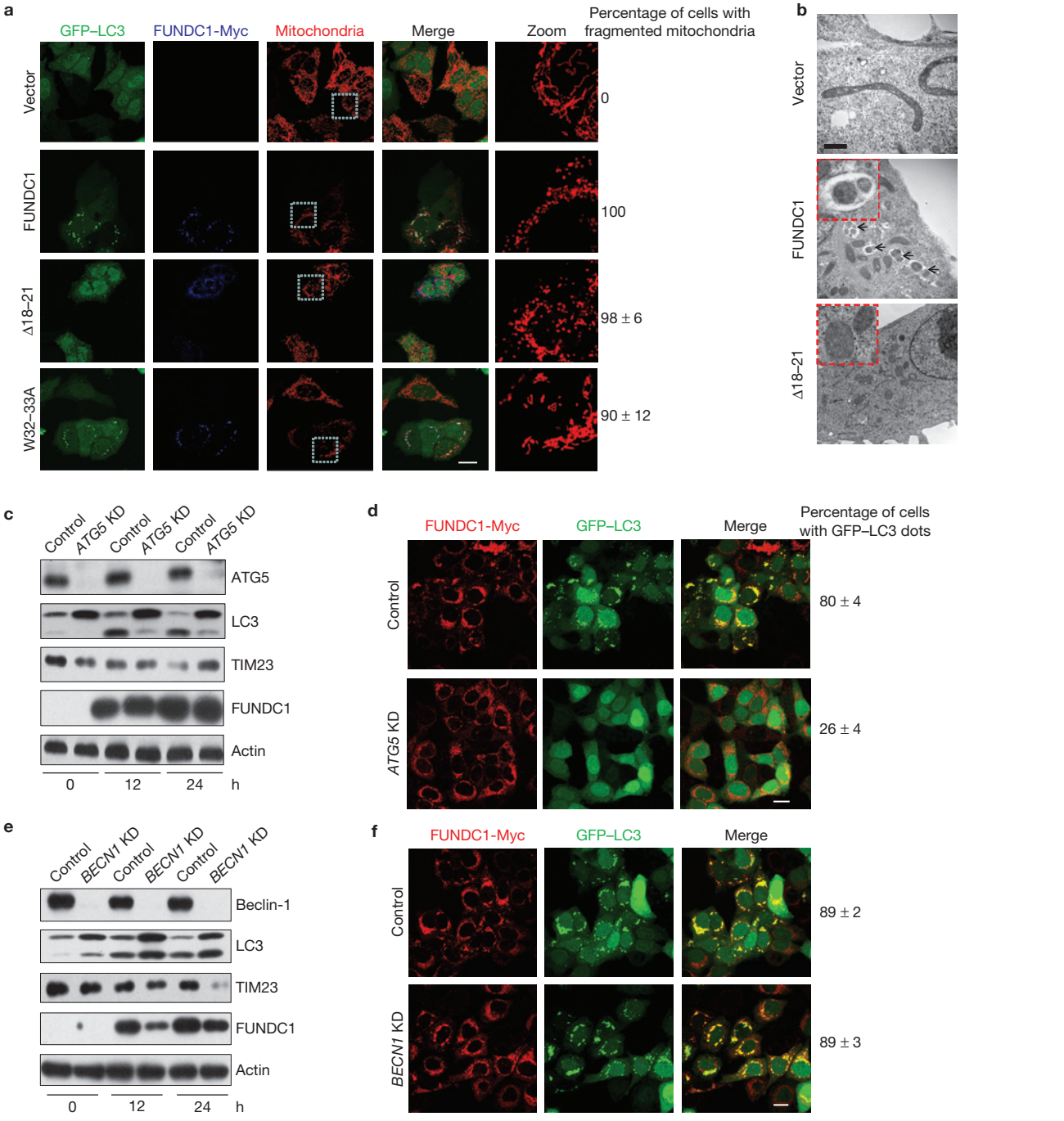

Figure 3 Deletion of LIR fails to induce mitophagy, which depends on ATG5, not on Beclin 1. (**a**) *FUNDC1*-knockdown HeLa cells were co-transfected with Myc vector and plasmids encoding FUNDC1–Myc, FUNDC1$^{\Delta 18-21}$, FUNDC1$^{W32-33A}$ (blue, anti-Myc) and GFP–LC3 for 24 h. The experiments were carried out as described in the caption of Fig. 2. Images show that the LIR-domain deletion mutant, but not the W32–33A mutant, failed to induce an increase in the number of GFP–LC3 dots although it induced mitochondrial fragmentation. Scale bar, 10 μm. The number of cells containing fragmented mitochondria was quantified (mean ± s.e.m.; $n = 100$ cells from three independent experiments). (**b**) *FUNDC1*-knockdown HeLa cells were co-transfected with Myc vector and plasmids encoding FUNDC1–Myc and FUNDC1$^{\Delta 18-21}$. After 24 h cells were processed and analysed by electron microscopy (black arrows, autophagic vacuoles). Scale bar, 600 nm. (**c**) Western blotting analysis of the LC3 and TIM23 expression in control cells and *ATG5*-knockdown (*ATG5* KD) cells that were transfected with plasmids encoding FUNDC1–Myc for 12 and 24 h. (**d**) Confocal microscopy was used to visualize the appearance of autophagosomes in control and *ATG5*-knockdown cells transfected with plasmids encoding FUNDC1 (red, anti-Myc) and GFP–LC3 (green) for 24 h. Scale bar, 10 μm. The numbers of autophagic cells were quantified (mean ± s.e.m.; $n = 100$ cells from three independent experiments). (**e**) Western blotting analysis of LC3 and TIM23 expression in control cells and *BECN1*-knockdown cells that were transfected with plasmids encoding FUNDC1–Myc for 12 and 24 h. (**f**) Confocal microscopy was used to visualize the appearance of autophagosomes in control and *BECN1*-knockdown cells transfected with plasmids encoding FUNDC1 (red, anti-Myc) and GFP–LC3 (green) for 24 h. Scale bar, 10 μm. Uncropped images of blots are shown in Supplementary Fig. S6.

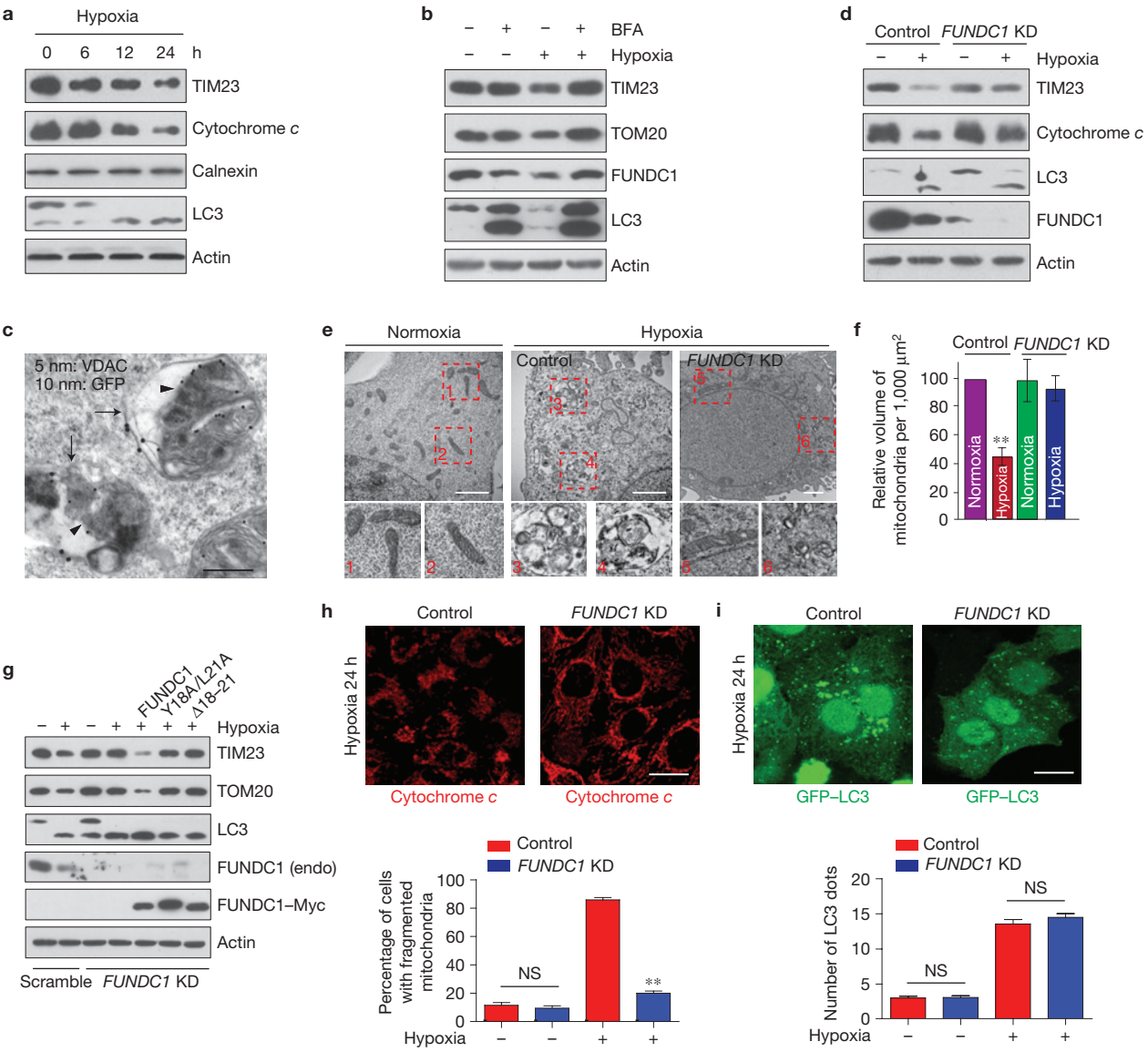

Figure 4 FUNDC1 mediates mitophagy induced by hypoxia. (**a**) HeLa cells were exposed to hypoxic conditions for the indicated times. TIM23, cytochrome *c*, calnexin and LC3 proteins were analysed by western blotting. (**b**) HeLa cells were treated with hypoxia for 0 and 12 h in the presence or absence of bafilomycin A1 (BFA); TIM23, TOM20, FUNDC1 and LC3 were detected by western blotting. (**c**) GFP–LC3 stable HeLa cells were maintained in hypoxic conditions for 24 h. Then samples were processed for immunogold electron microscopy with anti-VDAC1 antibodies (5 nm gold particles) to label mitochondria (arrowheads) and anti-GFP antibodies (10 nm gold particles) to label autophagosomes (arrows). Scale bar, 300 nm. (**d**) Control and *FUNDC1*-knockdown (KD) HeLa cells were treated with 1% O_2 for 0 or 18 h and analysed by western blotting with different antibodies. (**e**) Control HeLa cells and *FUNDC1*-knockdown stable HeLa cells were maintained in hypoxic conditions for 24 h or control HeLa cells were cultured under normoxia for 24 h. The samples were analysed by electron microscopy. Bars, 500 nm. (**f**) Control HeLa cells and *FUNDC1*-knockdown stable HeLa cells were grown in normoxia or exposed to 1% O_2 for 24 h. Cells were stained by TIM23. Three randomly picked regions of each sample were captured by confocal *z*-axis scanning and the total area of cells and volume of mitochondria were quantified (mean ± s.e.m.; $n = 90$ cells from three independent experiments). $^{**}P < 0.01$. (**g**) *FUNDC1*-knockdown cells were transfected with FUNDC1 or FUNDC1 mutants for 24 h and then exposed to hypoxic conditions for another 24 h. Samples were collected for western blotting. (**h**) Control and *FUNDC1*-knockdown cells were exposed to 1% O_2 for 24 h. Mitochondria were stained by cytochrome *c* antibody. The percentage of fragmented mitochondria was calculated (mean ± s.e.m.; $n = 100$ cells from three independent experiments). $^{**}P < 0.01$. (**i**) Control and *FUNDC1*-knockdown cells were transfected with GFP–LC3 for 24 h and then exposed to 1% O_2 for 0 or 24 h. The numbers of GFP–LC3 dots per cell were quantified (mean ± s.e.m.; $n = 100$ cells from three independent experiments). NS, not significant. Uncropped images of blots are shown in Supplementary Fig. S6.

(Supplementary Fig. S3d–g). Collectively, our data demonstrate that FUNDC1 mediates highly selective mitochondrial clearance under hypoxic conditions without impacting general autophagy.

The next question we addressed is how the interaction between FUNDC1 and LC3 is regulated in response to hypoxia. Mass spectrometric analysis revealed that Tyr 18 in the LIR motif of FUNDC1 was a potential phosphorylation site and its phosphorylation was diminished on hypoxia treatment (our unpublished observations). To confirm this observation, we raised an antibody specific for the phosphorylated Tyr 18 of FUNDC1. As shown in Fig. 5a, immunoblot

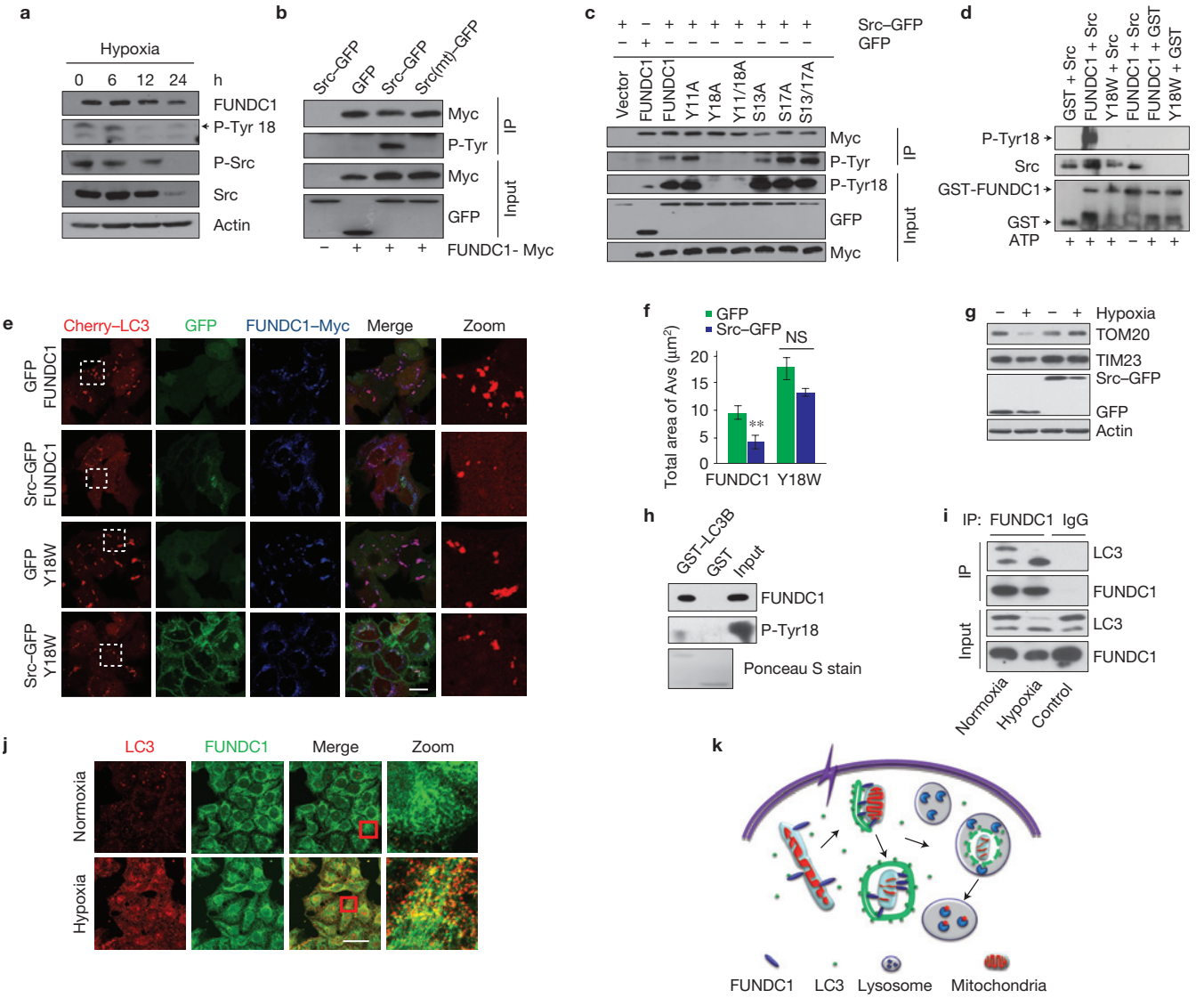

Figure 5 Dephosphorylation of FUNDC1 activates mitophagy induced by hypoxia. (**a**) The time course of the dephosphorylation of FUNDC1 and Src kinase on hypoxia as indicated by anti-p-FUNDC1 (Tyr 18) and anti-p-Src (Tyr 416) antibodies. (**b**) Plasmids encoding GFP, Src–GFP or Src(mt)–GFP (kinase dead) were co-transfected with plasmids encoding FUNDC1–Myc, and samples were immunoprecipitated (IP) by anti-Myc antibody and immunoblotted with anti-phosphotyrosine antibody. (**c**) HeLa cells were transfected with plasmids encoding Myc, FUNDC1–Myc and mutants in the presence of Src–GFP or GFP. Lysates were immunoprecipitated with anti-Myc antibody and immunoblotted with the indicated antibodies. (**d**) *In vitro* kinase assay: GST, GST–FUNDC1 or GST–FUNDC1^{Y18W} was incubated for 20 min with or without Src and then samples were analysed by western blotting. (**e**) Cherry–LC3-positive *FUNDC1*-knockdown cells were co-transfected with plasmids encoding FUNDC1 or FUNDC1^{Y18W} in the presence of Src–GFP or GFP for 24 h. Representative confocal microscopy images are shown. Scale bar, 20 μm. (**f**) The total area of autophagosomes (AVs) was quantified (mean ± s.e.m.; $n = 200$ cells from three independent experiments). $^{**}P < 0.01$. NS, not significant. (**g**) HeLa cells transfected with plasmids encoding GFP or Src–GFP were maintained in hypoxic conditions or left in normoxic conditions for 12 h. Cells were analysed by western blotting. (**h**) FUNDC1–Myc transfectant lysates were incubated with immobilized GST or GST–LC3B beads and detected by western blotting. Ponceau S was used to visualize GST and GST–LC3B. (**i**) HeLa cells were exposed to normoxic or hypoxic conditions for 24 h. Endogenous LC3 were immunoprecipitated with anti-FUNDC1 antibody or IgG. Samples were analysed by western blotting. (**j**) HeLa cells were treated with hypoxia or normoxia. Samples were visualized by immunofluorescence with anti-LC3 (red) and anti-FUNDC1 (green) antibodies. Scale bar, 20 μm. (**k**) Hypothetical model of FUNDC1 in mitophagy in response to hypoxia. FUNDC1 is phosphorylated at Tyr 18 under normoxia by Src tyrosine kinase and dephosphorylated under hypoxic conditions. This increases its binding to LC3-II, which is abundantly produced under hypoxia treatment. The recruitment of LC3-bound isolation membrane will lead to the expansion of the isolation membrane around the mitochondrion to form the autophagosome, which is then fused with lysosomes for degradation. Uncropped images of blots are shown in Supplementary Fig. S6.

analysis revealed that endogenous FUNDC1 in the cells is indeed present as a phosphorylated form under normoxia conditions; however, on hypoxia treatment, the level of phosphorylated FUNDC1 was markedly reduced. Computational analysis predicts that the Src kinase may be responsible for the Tyr 18 phosphorylation of FUNDC1 (refs 29,30). It is well known that several members of the Src family of kinases are localized in mitochondria[31,32]. We found that the inactivation of Src kinase, indicated by the dephosphorylation of

Tyr 416 (ref. 33), is closely correlated with the dephosphorylation of FUNDC1 and the occurrence of mitophagy on hypoxia treatment (Fig. 5a). Indeed, we discovered that an active Src kinase, but not its kinase-dead form, was able to phosphorylate FUNDC1 at Tyr 18, but not at Tyr 11, Ser 13 or Ser 17 (Fig. 5b,c). Incubation of FUNDC1 and its mutant Y18W with Src kinase further demonstrated that FUNDC1 is a direct substrate of Src kinase (Fig. 5d). Ectopic expression of wild-type Src could significantly block the Cherry–LC3 punctum formation induced by wild-type FUNDC1, but not by Y18W, a mutant of FUNDC1 that cannot be phosphorylated (Fig. 5e,f). Moreover, Src kinase inhibits FUNDC1-mediated mitophagy in response to hypoxia (Fig. 5g). LC3 preferentially binds the dephosphorylated FUNDC1 (Fig. 5h), and hypoxia treatment, which induces dephosphoryation of FUNDC1, results in an increase of the co-localization and interaction between FUNDC1 and LC3-II (Fig. 5i,j). These data indicate that dephosphorylation of FUNDC1 triggers the activation of mitophagy in response to hypoxia.

Our data demonstrate that FUNDC1 is a receptor of selective mitophagy in response to hypoxia through its characteristic LIR to specifically interact with LC3. Under normal physiological conditions, FUNDC1-mediated mitophagy is inhibited by its phosphorylation at the Tyr 18 position in the LIR motif by Src kinase. On hypoxia stimulation, Src is inactivated and FUNDC1 is dephosphorylated, resulting in an increase of the co-localization and interaction between FUNDC1 and LC3-II, leading to the selective incorporation of the mitochondrion as a specific cargo into LC3-bound isolation membrane for subsequent removal of mitochondria by LAMP1-positive autolysosomes (Fig. 5k). Our findings thus provide insights into how FUNDC1 acts as a mitophagy receptor to couple with the core autophagic machinery[34] and how FUNDC1-dependent mitophagy is regulated by the Src kinase pathway, although the exact molecular mechanisms need further investigation. Previous studies have shown that Atg32 interacts with Atg8 through its LIR motif for highly specific mitophagy in yeast[19,20]. The expression of both Atg32 and FUNDC1 is reduced during mitophagy[20] (Fig. 5 and Supplementary Fig. S4b,c). Furthermore, Atg32 is also found to be phosphorylated at Ser 114, although the kinase responsible for this modification has yet to be identified[35].

Deletion of the FUNDC1 LIR resulted in defects in the autophagosome membrane formation, but failed to induce mitophagy, although the mutant was able to cause mitochondrial fragmentation as wild-type FUNDC1 did (Figs 2 and 3). Mitochondrial fragmentation may be a prerequisite, but not sufficient, for the autophagosome formation. Knockdown of *FUNDC1* reduces the recruitment of LC3 towards mitochondria and prevents mitochondrial fragmentation under hypoxia, thus decreasing the levels of mitophagy. FUNDC1 is conserved in higher eukaryotic organisms and highly expressed in most tissues (Supplementary Fig. S4a), indicating that the mechanism of mitophagy is important for cellular functions.

Nix is involved in hypoxia-induced autophagy and is indispensable for programmed elimination of mitochondria during reticulocyte maturation[15,27,36]. Obviously, the mechanism of FUNDC1-induced mitophagy is distinct from that of Nix or its homologue BNIP3 on the basis of our findings. For example, unlike FUNDC1, Nix shows much weaker binding with LC3B whereas the conversion of LC3B is correlated with elevated levels of autophagic vesicles in response to autophagy-inducing stress[37,38]. Clearly, knockdown of *FUNDC1* did not affect the distribution of BNIP3 towards mitochondria (Supplementary Fig. S5a). In addition, although both are found to be involved in mitophagy induced by hypoxia, an increased expression of Nix or BNIP3 was observed whereas the level of FUNDC1 was decreased. Furthermore, Nix and BNIP3 are localized at other organelles and are involved in regulating apoptotic or programmed necrosis through affecting mitochondrial respiration[27,39,40]. Apparently, FUNDC1 does not impact cell viability under the hypoxic condition after *FUNDC1* is knocked down (Supplementary Fig. S5b–d). Taken together, the roles of FUNDC1 and BNIP3 in the induction of mitophagy are different, although we cannot rule out the possibility of their cooperation for mitophagy. □

METHODS

Methods and any associated references are available in the online version of the paper at http://www.nature.com/naturecellbiology

Note: Supplementary Information is available on the Nature Cell Biology website

ACKNOWLEDGEMENTS

We wish to thank H. Zhang from the National Institute of Biological Sciences, China, and L. Yu from Tsinghua University, China, for their suggestions and critical reading of the manuscript. We thank Y. G. Chen from Tsinghua University for providing PGEX4T1-GABARAP and PGEX4T1-GABARAPL2 constructs. We wish to thank M. Bartlam from Nankai University and A. Zhou from Cleveland State University in Ohio for improvement of the English of the manuscript. The Chen laboratory was supported by the 973 project of the Ministry of Science and Technology (China) (2011CB910903 and 2010CB912204) and by grants from the National Natural Science Foundation of China (81130045, 90713006).

AUTHOR CONTRIBUTIONS

L.L. observed that FUNDC1 could potentially induce mitophagy and carried out most of the biochemistry experiments. D.F. designed and carried out all electron microscopy analysis in S.S.'s laboratory. D.F. and G.C. identified that FUNDC1 is a substrate of Src kinase with some help from W.Q. D.F. and P.X. analysed the phosphorylation sites of FUNDC1 by mass spectrometry in F.Y.'s laboratory. D.F. and L.H. carried out the three-dimensional reconstruction and mitochondrial volume calculations. Q.Z. carried out fractionation analysis in P.L.'s laboratory. C.Z. and M.C. carried out cell-viability analysis. L.L., D.F. and Q.C. analysed and organized the data. Q.C. wrote the manuscript with input from L.L. and D.F. All authors discussed the results and commented on the manuscript.

COMPETING FINANCIAL INTERESTS

The authors declare no competing financial interests.

Published online at http://www.nature.com/naturecellbiology
Reprints and permissions information is available online at http://www.nature.com/reprints

1. Wallace, D. C. A mitochondrial paradigm of metabolic and degenerative diseases, aging, and cancer: a dawn for evolutionary medicine. *Annu. Rev. Genet.* **39,** 359–407 (2005).
2. Lin, M. T. & Beal, M. F. Mitochondrial dysfunction and oxidative stress in neurodegenerative diseases. *Nature* **443,** 787–795 (2006).
3. Goldman, S. J., Taylor, R., Zhang, Y. & Jin, S. Autophagy and the degradation of mitochondria. *Mitochondrion* **10,** 309–315 (2010).
4. Narendra, D., Tanaka, A., Suen, D. F. & Youle, R. J. Parkin is recruited selectively to impaired mitochondria and promotes their autophagy. *J. Cell Biol.* **183,** 795–803 (2008).
5. Mizushima, N., Levine, B., Cuervo, A. M. & Klionsky, D. J. Autophagy fights disease through cellular self-digestion. *Nature* **451,** 1069–1075 (2008).
6. Levine, B. & Kroemer, G. Autophagy in the pathogenesis of disease. *Cell* **132,** 27–42 (2008).
7. Mizushima, N., Ohsumi, Y. & Yoshimori, T. Autophagosome formation in mammalian cells. *Cell Struct. Funct.* **27,** 421–429 (2002).
8. Lemasters, J. J. Selective mitochondrial autophagy, or mitophagy, as a targeted defense against oxidative stress, mitochondrial dysfunction, and aging. *Rejuvenation Res.* **8,** 3–5 (2005).
9. Youle, R. J. & Narendra, D. P. Mechanisms of mitophagy. *Nat. Rev. Mol. Cell Biol.* **12,** 9–14 (2011).

10. Twig, G. *et al.* Fission and selective fusion govern mitochondrial segregation and elimination by autophagy. *EMBO J.* **27,** 433–446 (2008).
11. Narendra, D. P. *et al.* PINK1 is selectively stabilized on impaired mitochondria to activate Parkin. *PLoS Biol.* **8,** e1000298 (2010).
12. Vives-Bauza, C. *et al.* PINK1-dependent recruitment of Parkin to mitochondria in mitophagy. *Proc. Natl Acad. Sci. USA* **107,** 378–383 (2010).
13. Geisler, S. *et al.* PINK1/Parkin-mediated mitophagy is dependent on VDAC1 and p62/SQSTM1. *Nat. Cell Biol.* **12,** 119–131 (2010).
14. Kitada, T. *et al.* Mutations in the *parkin* gene cause autosomal recessive juvenile parkinsonism. *Nature* **392,** 605–608 (1998).
15. Sandoval, H. *et al.* Essential role for Nix in autophagic maturation of erythroid cells. *Nature* **454,** 232–235 (2008).
16. Schweers, R. L. *et al.* NIX is required for programmed mitochondrial clearance during reticulocyte maturation. *Proc. Natl Acad. Sci. USA* **104,** 19500–19505 (2007).
17. Ichimura, Y. *et al.* A ubiquitin-like system mediates protein lipidation. *Nature* **408,** 488–492 (2000).
18. Kabeya, Y. *et al.* LC3, a mammalian homologue of yeast Apg8p, is localized in autophagosome membranes after processing. *EMBO J.* **19,** 5720–5728 (2000).
19. Kanki, T., Wang, K., Cao, Y., Baba, M. & Klionsky, D. J. Atg32 is a mitochondrial protein that confers selectivity during mitophagy. *Dev. Cell* **17,** 98–109 (2009).
20. Okamoto, K., Kondo-Okamoto, N. & Ohsumi, Y. Mitochondria-anchored receptor Atg32 mediates degradation of mitochondria via selective autophagy. *Dev. Cell* **17,** 87–97 (2009).
21. Rubinsztein, D. C. *et al.* In search of an 'autophagomometer'. *Autophagy* **5,** 585–589 (2009).
22. Pankiv, S. *et al.* p62/SQSTM1 binds directly to Atg8/LC3 to facilitate degradation of ubiquitinated protein aggregates by autophagy. *J. Biol. Chem.* **282,** 24131–24145 (2007).
23. Noda, N. N., Ohsumi, Y. & Inagaki, F. Atg8-family interacting motif crucial for selective autophagy. *FEBS Lett.* **584,** 1379–1385 (2010).
24. Gao, P. *et al.* The Bcl-2 homology domain 3 mimetic gossypol induces both Beclin 1-dependent and Beclin 1-independent cytoprotective autophagy in cancer cells. *J. Biol. Chem.* **285,** 25570–25581 (2010).
25. Zhao, L. *et al.* Morphine induces Beclin 1- and ATG5-dependent autophagy in human neuroblastoma SH-SY5Y cells and in the rat hippocampus. *Autophagy* **6,** 386–394 (2010).
26. Zhu, Y. *et al.* Beclin 1 cleavage by caspase-3 inactivates autophagy and promotes apoptosis. *Protein Cell* **1,** 468–477 (2010).
27. Bellot, G. *et al.* Hypoxia-induced autophagy is mediated through hypoxia-inducible factor induction of BNIP3 and BNIP3L via their BH3 domains. *Mol. Cell Biol.* **29,** 2570–2581 (2009).
28. Zhang, H. *et al.* Mitochondrial autophagy is an HIF-1-dependent adaptive metabolic response to hypoxia. *J. Biol. Chem.* **283,** 10892–10903 (2008).
29. Xue, Y. *et al.* GPS 2.0, a tool to predict kinase-specific phosphorylation sites in hierarchy. *Mol. Cell. Proteomics* **7,** 1598–1608 (2008).
30. Huang, H. D., Lee, T. Y., Tzeng, S. W. & Horng, J. T. KinasePhos: a web tool for identifying protein kinase-specific phosphorylation sites. *Nucleic Acids Res.* **33,** W226–W229 (2005).
31. Arachiche, A. *et al.* Localization of PTP-1B, SHP-2, and Src exclusively in rat brain mitochondria and functional consequences. *J. Biol. Chem.* **283,** 24406–24411 (2008).
32. Miyazaki, T., Neff, L., Tanaka, S., Horne, W. C. & Baron, R. Regulation of cytochrome *c* oxidase activity by c-Src in osteoclasts. *J. Cell Biol.* **160,** 709–718 (2003).
33. Thomas, S. M. & Brugge, J. S. Cellular functions regulated by Src family kinases. *Annu. Rev. Cell Dev. Biol.* **13,** 513–609 (1997).
34. Yang, Z. & Klionsky, D. J. An overview of the molecular mechanism of autophagy. *Curr. Top. Microbiol. Immunol.* **335,** 1–32 (2009).
35. Aoki, Y. *et al.* Phosphorylation of Serine 114 on Atg32 mediates mitophagy. *Mol. Biol. Cell.* **22,** 3206–3217 (2011).
36. Novak, I. & Dikic, I. Autophagy receptors in developmental clearance of mitochondria. *Autophagy* **7,** 301–303 (2011).
37. Novak, I. *et al.* Nix is a selective autophagy receptor for mitochondrial clearance. *EMBO Rep.* **11,** 45–51 (2010).
38. Klionsky, D. J. *et al.* Guidelines for the use and interpretation of assays for monitoring autophagy in higher eukaryotes. *Autophagy* **4,** 151–175 (2008).
39. Chen, Y. *et al.* Dual autonomous mitochondrial cell death pathways are activated by Nix/BNip3L and induce cardiomyopathy. *Proc. Natl Acad. Sci. USA* **107,** 9035–9042 (2010).
40. Rikka, S. *et al.* Bnip3 impairs mitochondrial bioenergetics and stimulates mitochondrial turnover. *Cell Death Differ.* **18,** 721–731 (2011).

DOI: 10.1038/ncb2422

METHODS

Animals, reagents and antibodies. All mice were maintained and cared for on the basis of animal protocols approved by the Institutional Animal Care Committee. Adult C57BL/6(B6) mice were treated in either normoxic or 8% hypoxic conditions in a hypoxia chamber for 72 h, and then brain tissues were prepared and mitochondrial proteins such as TIM23, FIS1, MFN1 and FUNDC1 were examined by western blotting.

The following antibodies were used: anti-TIM23 (1:1,000), anti-TOM20 1:1,000 (BD Biosciences), anti-GFP (1:2,000, monoclonal; Santa Cruz), anti-cytochrome *c* (1:1,000), anti-beclin-1 (1:1,000), anti-calnexin monoclonal antibody (1:1,000), anti-GM130 monoclonal antibody (1:1,000; BD Biosciences); anti-LC3B polyclonal antibody (1:1,000), anti-actin monoclonal antibody (1:10,000; Sigma); anti-c-Myc monoclonal antibody (1:1,000; Santa Cruz); anti-FUNDC1 polyclonal antibody (1:1,000; AVIVA); anti-GFP polyclonal antibody (1:2,000; Invitrogen); anti-VDAC1 monoclonal antibody (1:2,000), anti-Bnip3 polyclonal antibody (1:1,000; Abcam); anti-Src (1:1,000) and anti-Src(Tyr 416) polyclonal antibody (1:1,000; Cell Signaling); anti-GST (1:3,000); anti-p-FUNDC1 (Tyr 18) polyclonal antibody (1:1,000) was generated by immunizing rabbits with purified phosphopeptides in FUNDC1 and affinity purified (Abgent). The following fluorescent secondary antibodies were used: goat anti-mouse IgG fluorescein isothiocyanate (FITC), Cy3 (DAKO); goat anti-rabbit IgG (DAKO); goat anti-mouse Cy5 (Invitrogen). Polyclonal antibodies against FUNDC1 were generated by immunizing rabbits with recombinant FUNDC1 (δ transmembrane domain) protein produced in *Escherichia coli* using pET28a expression vector. For immunoprecipitation assay, anti-GFP polyclonal antibody 1:1,000 (Invitrogen), anti-FUNDC1 1:1,000, anti-Myc 1:100; for immunofluorescence, anti-TIM23 1:100, anti-TOM20 1:100, anti-cytochrome *c* 1:100, anti-Myc 1:100, anti-FUNDC1 1:50, anti-LC3B (nanotools) 1:50. The following fluorescent secondary antibodies were used: goat anti-mouse IgG FITC 1:100; goat anti-mouse IgG Cy3 1:100; goat anti-rabbit IgG FITC (DAKO) 1:100; goat anti-mouse Cy5 (Invitrogen) 1:100. Bafilomycin A1 and neomycin were purchased from Sigma. Immunogold antibodies (1:50) were purchased from the Jackson Laboratory and Sigma.

Cell culture and transfection. HeLa cells were grown in DMEM supplemented with 10% fetal bovine serum (Hyclone) and 1% penicillin–streptomycin at 37 °C under 5% CO_2. Hypoxic conditions were achieved with a hypoxia chamber (Billups-Rothenberg) flushed with a preanalysed gas mixture of 1% O_2, 5% CO_2 and 95% N_2. The target sequence in FUNDC1 for RNA interference is 5′-GCAGCACCTGAAATCAACA-3′; the target sequence in ATG5 is 5′-GAAGTTTGTCCTTCTGCTA-3′; the scramble RNA interference sequence is 3′-GACATTTGTAACGGGATTC-5′; the target sequence in beclin-1 for RNA interference is 5′-CTCAGGAGAGGAGCCATTT-3′. Primers for short hairpin RNA were designed according to the manufacturer's instructions (Ambion), and cloned into the pSilencer2.1-neo vector. To establish stable cell lines, HeLa cells were transfected with the corresponding vectors and selected with neomycin.

Real-time PCR analysis. RNA was prepared using TRIzol reagent (Invitrogen). Complementary DNA was synthesized using the SuperScript VILO cDNA synthesis kit (Invitrogen). Real-time PCR was carried out by using a Quant One Step qRT–PCR (Probe) Kit (Tiangen) and a CFX96 real-time PCR detection system (Applied Biosystems). For semiquantitive PCR, primers were as follows: FUNDC1 5′-ATGGCATCCCGGAACCCCC-3′ (forward) and 5′-AGATGCCAGGCCTAGCAAAAAG-3′ (reverse), 5′-HPRTCACAGGACTAGAACACCTGC-3′ (forward) and 5′-GCTGGTGAAAAGGACCTCT-3′ (reverse). For real-time PCR primers were as follows: FUNDC1 5′-GCAGTAGGTGGTGGCTTTC-3′ (forward) and 5′-TGCTTTGTTCGCTCGTTT-3′ (reverse), 5′-GAPDHTGCACCACCAACTGCTTAGC-3′ (forward) and 5′-TCTTCTGGGTGGCAGTGATG-3′ (reverse).

Cell viability assay. Apoptotic events were evaluated by annexin V labelling, using the annexin V-fluorescein isothiocyanate/propidium iodide assay kit (BD Biosciences) according to the standard protocol. The LDH activity was detected with a commercial LDH assay kit (Jiancheng BioEngineering) according to the manufacturer's instructions.

Immunofluorescence microscopy. Cells were grown to 60% confluence on a coverslip. After treatment, cells were washed twice with PBS, and fixed with freshly prepared 3.7% formaldehyde at 37 °C for 15 min. Antigen accessibility was increased by treatment with 0.2% Triton X-100. Cells were incubated with primary antibodies for 1 h, and, after washing with PBS, stained with a secondary antibody for a further 45 min. Cell images were captured with an LSM 510 Zeiss confocal microscope.

Electron microscopy. Cells were grown and treated as described above. For immunoelectron microscopy, cells were first fixed with 2% paraformaldehyde and 0.2% glutaraldehyde in Na cacodylate buffer (pH 7.4) at 37 °C for 2 h, and then dehydrated in a graded ethanol series and embedded in acrylic resin (LR White). 70 nm ultrathin sections were mounted on nickel grids, incubated with 1% BSA/PBS and incubated overnight at 4 °C with a mixture of primary antibodies (anti-GFP antibody (dilution 1/200) and/or anti-VDAC1 antibody at final concentration 2 μg ml^{-1}) in 1% BSA/PBS, washed five times for 5 min in 0.5% BSA/PBS and then labelled for 2 h with 5 nm (or 20 nm) goat anti-mouse for VDAC1 and 10 nm goat anti-rabbit for GFP–LC3 gold-conjugated particles in 1% BSA/PBS. Grids were finally washed four times for 5 min in 0.5% BSA/PBS, incubated for 15 min in 1% glutaraldehyde/PBS, washed twice for 5 min in PBS and three times in distilled water, stained and dried at room temperature. The samples were visualized using a 120 kV Jeol electron microscope at 80 kV and images were captured using an AMT digital camera.

SDS–PAGE and western blotting. Cells or membrane fractions were lysed in lysis buffer (20 mM Tris, pH 7.4, 2 mM EGTA, 1% NP-40, protease inhibitors). Equivalent protein quantities (20 μg) were subjected to SDS–PAGE, and transferred to nitrocellulose membranes. Membranes were probed with the indicated primary antibodies, followed by the appropriate HRP-conjugated secondary antibodies (KPL). Immunoreactive bands were visualized with a chemiluminescence kit (Pierce).

Immunoprecipitation. HeLa cells were transiently transfected using the calcium phosphate method. At 24 h post transfection, the cells were lysed with 0.5 ml of lysis buffer plus protease inhibitors (Roche Applied Science) for 30 min on ice. After 12,000 *g* centrifugation for 15 min, the lysates were immunoprecipitated with specific antibody and Protein A-Sepharose (Invitrogen) overnight at 4 °C. Thereafter, the precipitants were washed three times with lysis buffer, and the immune complexes were eluted with sample buffer containing 1% SDS for 5 min at 95 °C and analysed by SDS–PAGE.

GST pulldown. All GST tagged proteins were expressed in *E. coli* BL21(DE3). GST fusion proteins were purified on glutathione–Sepharose 4 Fast Flow beads (Amersham Biosciences). For GST pulldown with purified FUNDC1 protein, 4 μg of GST–LC3B protein was incubated with 1 μg of FUNDC1 protein in 500 μl PBS buffer for 2 h at 4 °C and then washed five times with 1 ml of PBS buffer. For GST pulldown with HeLa cell lysates, 4 μg of GST fusion proteins were incubated with 1,000 μg of HeLa cell lysate for 2 h at 4 °C and then washed five times with 1 ml of lysis buffer. The precipitate complex was boiled with sample buffer containing 1% SDS for 5 min at 95 °C and analysed by SDS–PAGE. The nitrocellulose membrane was stained with Ponceau S, followed by immunoblotting with anti-FUNDC1 antibody.

Subcellular fractionation. Cells were collected and resuspended in hypotonic buffer. After gentle homogenization with a Dounce homogenizer, cell lysates were subjected to differential centrifugation and gradient centrifugation. The resulting membrane fractions were lysed, and analysed by western blotting.

Protease protection assay. For proteinase K digestion, isolated mitochondria were suspended in hypotonic buffer and incubated on ice with 10 μg ml^{-1} proteinase K (Sigma) containing the indicated concentrations of digitonin (Sigma) or 1% Triton X-100 for 30 min. Digestion was terminated with 2 mM phenylmethyl sulphonyl fluoride (Sigma) (final concentration). Mitochondrial proteins were separated by SDS–PAGE and proteins were detected by western blotting with the indicated antibodies.

Three-dimensional surface reconstruction and mitochondrial volume calculations. Three-dimensional surface-reconstruction image raw data sets were collected by spinning-disc confocal microscopy. The Z-Stack was deconvolved and three-dimensional surface reconstruction was carried out with IMARIS7.0.0 software (Bitplane).

All confocal microscopy was carried out on an LSM 510 spectral confocal microscope (Zeiss). Confocal slice thickness was typically kept at 0.6 μm consistently for each fluorescence channel, with ten slices typically being taken to encompass the three-dimensional entirety of the cells in the field of view. Maximum-intensity projections of each region were calculated for subsequent quantification and analysis. To quantify mitochondrial volume, images were deconvolved with ImageJ (NIH) and Z-Stack analysis of the thresholded images volume-reconstituted using the VolumeJ plug-in, and volumes of mitochondria were quantified using the ImageJ-3D Object Counter plug-in. Care was taken to ensure consistency of thresholding over multiple fields of view and samples. Once this process was complete, Object Counter 3D under the particle analysis algorithm within ImageJ was employed to measure the volume of mitochondria and area of cells within a specified region of interest. Calculation for the adjusted total mitochondrial volume per cell was as follows: (percentage of total volume of mitochondria)/(percentage of total area of cell). This process was completed for at least 90 cells over three separate fields of view for each sample and is representative of three independent experiments.

Statistical analysis. In quantitative analyses using cultured cells represented as histograms, values were obtained from three independent experiments, and expressed as means ± s.e.m. Statistical analysis was carried out using the Student *t*-test, with *P* values <0.05 considered significant. $^{*}P < 0.05$ and $^{**}P < 0.01$ versus the corresponding controls are indicated. All statistical data were calculated with the GraphPad Prism software.

DOI: 10.1038/ncb2422

nature cell biology

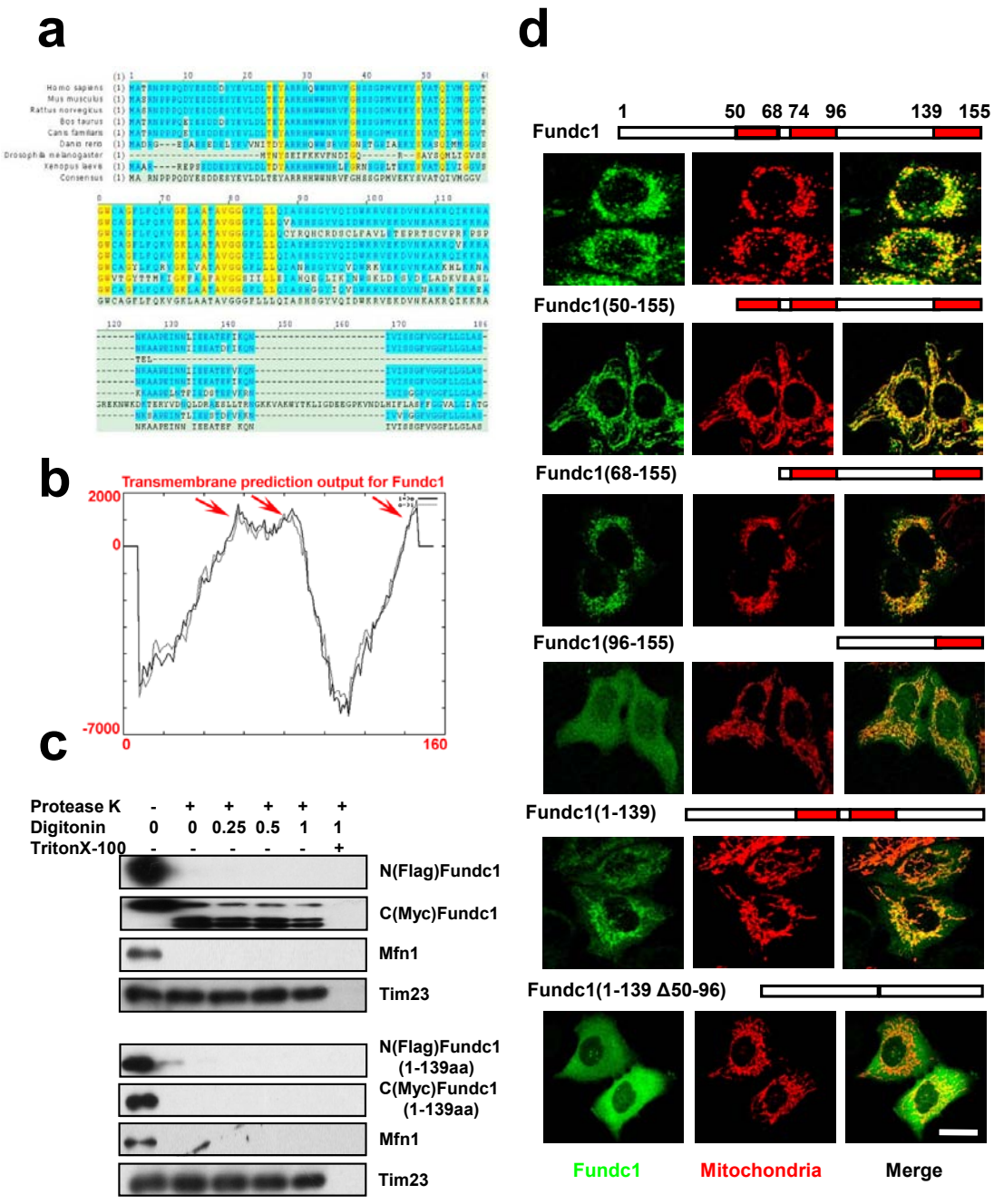

Figure S1 The topology of Fundc1. (a) Amino acid sequences of Fundc1 proteins from different species were aligned using the VectorNTI program. (b) Hydrophobicity plot for Fundc1 was measured by the TMpred algorithm showing probability for transmembrane domains. (c) HeLa cells were transfected with (Flag)N-Fundc1(1-155)-C(Myc) or (Flag)N-Fundc1(1-139)-C(Myc) vectors, respectively. Cells were then dounce homogenized and the isolated mitochondria were treated with proteinase K in the presence or absence of digitonin or TritonX-100. Western blotting was carried out with anti-Myc, anti-Flag, anti-Mfn1(mitochondrial outer membrane protein) and anti Tim23 (mitochondrial inner membrane protein). (d) Representative immunofluorescence images of transiently transfected HeLa cells expressing wild-type and indicated truncated Fundc1. The distribution of Fundc1 (green, anti-Myc) and mitochondria (red, mito-dsRed) were then visualized by confocal microscopy. Bar, 10 μm.

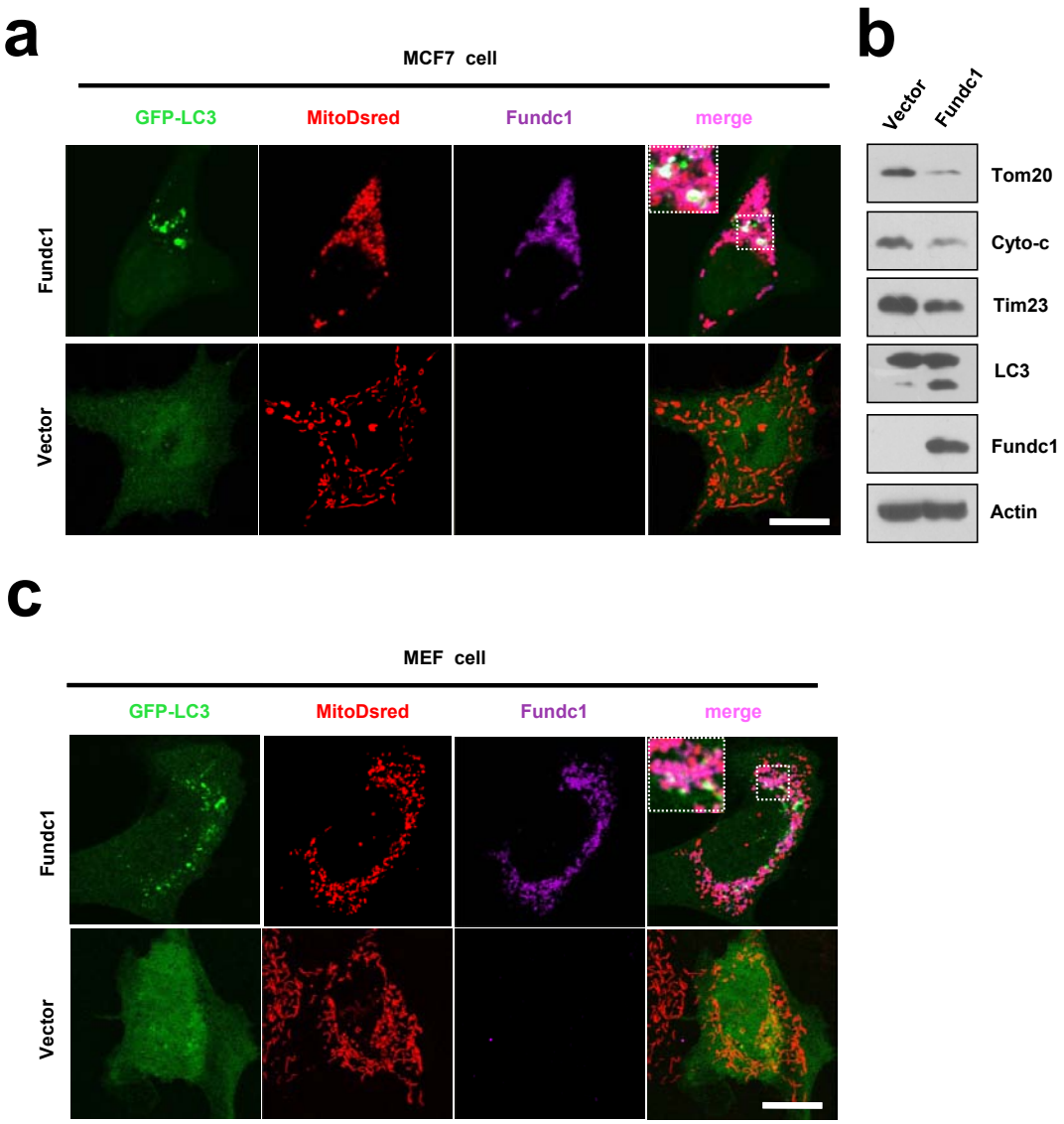

Figure S2 Fundc1 could induce mitophagy both in MCF7 and primary MEF cells. (a) GFP-LC3 stable MCF7 cells were transfected with Fundc1-myc and Mito-dsRed for 24 h. The cells were then fixed and immunostained with Fundc1 (purple, anti-Myc) before visualization by confocal microscopy for GFP-LC3 (Green) and mitochondria (red, mito-dsRed). Bar, 10 μm. (b) MCF cells were transfected with vector or Fundc1-myc for 24 h and then were harvested for Western blotting with indicated antibodies. (c) Primary MEFs were transfected with Fundc1-myc and Mito-dsRed for 24 h. The cells were then fixed and immunostained with Fundc1 (purple, anti-Myc) before visualization by confocal microscopy for GFP-LC3 (Green) and mitochondria (red, mito-dsRed). Bar, 10 μm.

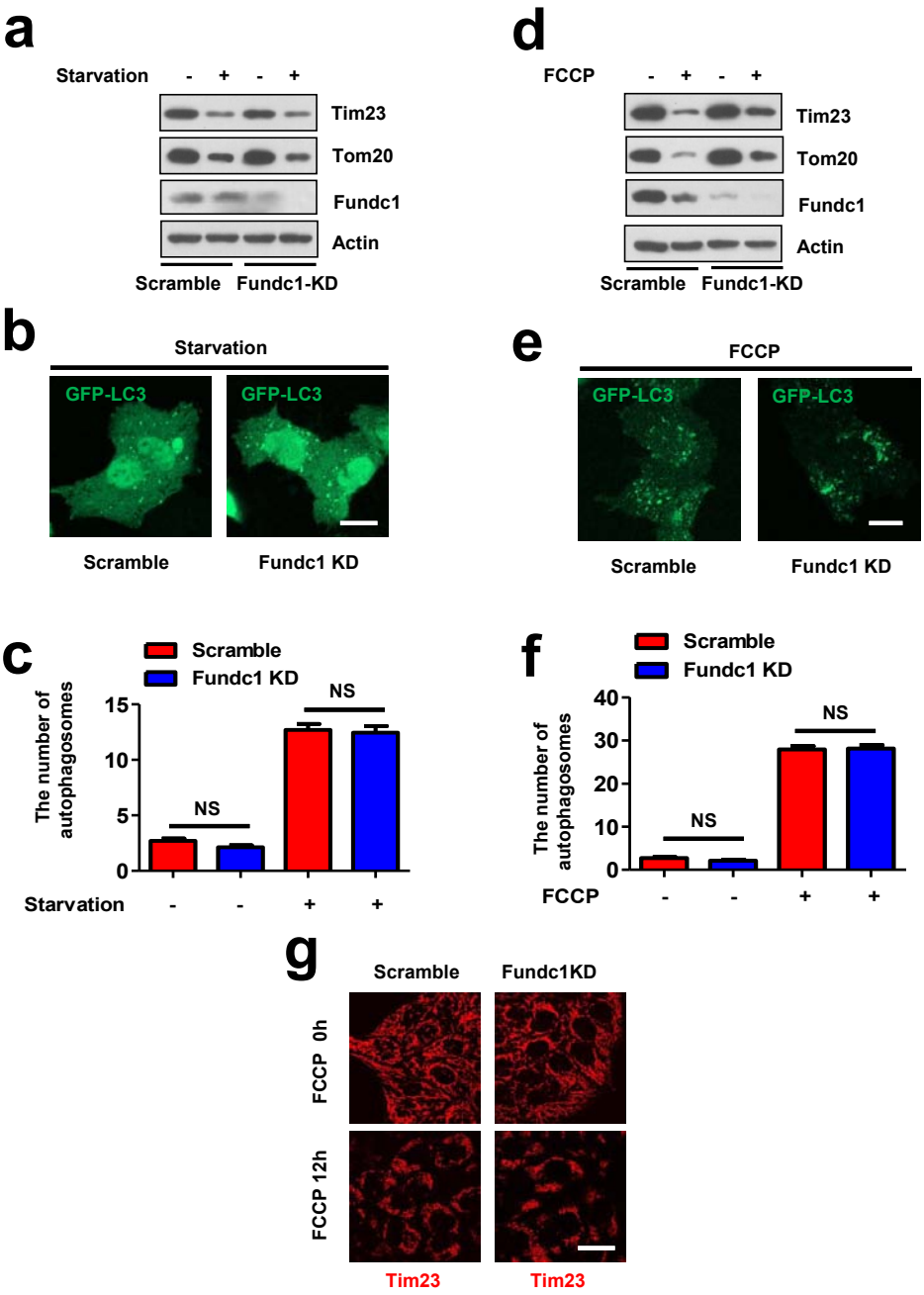

Figure S3 The effects of Fundc1 knockdown on starvation and FCCP induced autophagy/mitophagy. (a). Control and Fundc1 knockdown cells were subjected to starvation for 10 h and then analyzed for the expression of mitochondrial proteins by Western blotting. (b, c) Control and Fundc1 knockdown cells were transfected with GFP-LC3 for 24 h and then subjected to starvation for 10 h. Bar, 10 μm. The numbers of GFP-LC3 dots per cells were quantified (mean ± s.e.m.; n=100 cells from three independent experiments). NS, not significant. (d) Control and Fundc1 knockdown cells were treated with 10 μM FCCP for 12 h and analyzed for the expression of mitochondrial proteins by Western blotting. (e, f) Control and Fundc1 knockdown cells were transfected with GFP-LC3 for 24 h and subjected to the treatment of FCCP (10 μM) for 12 h. Bar, 10 μm. The numbers of GFP-LC3 dots per cells were quantified (mean ± s.e.m.; n = 100 cells from three independent experiments). NS, not significant. (g) Control and Fundc1 knockdown cells were treated with 10 μM FCCP for 12 h. Mitochondria were stained by Tim23 antibody (red). Bar, 10 μm. The mitochondria in the control and Fundc1 KD cells were all fragmented.

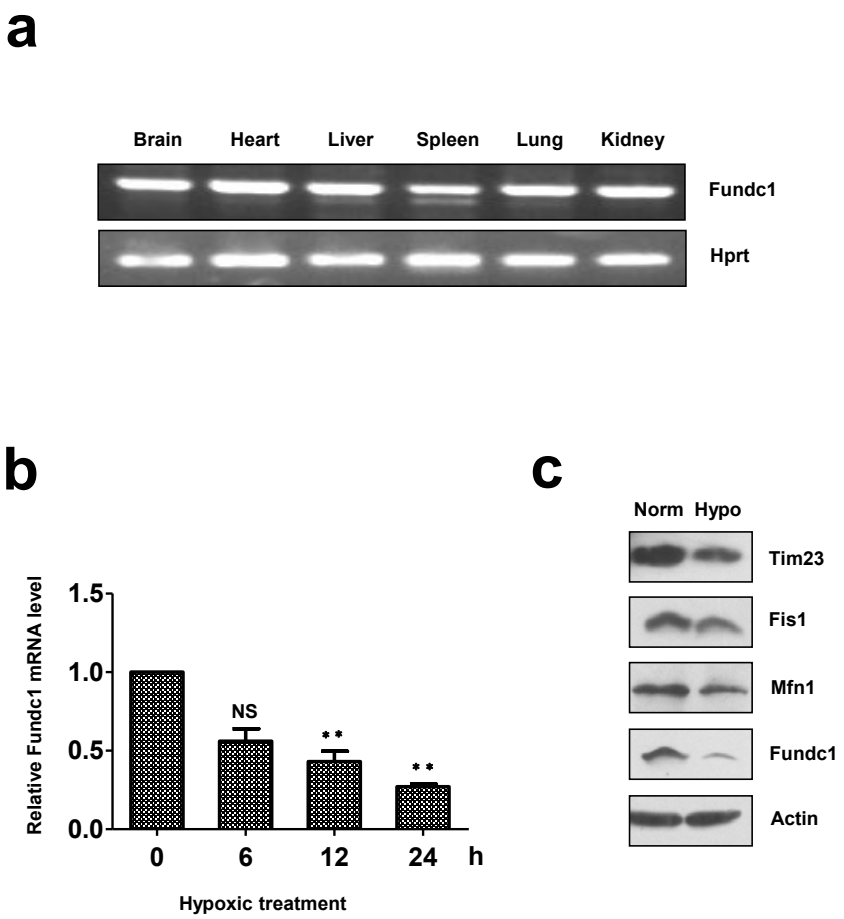

Figure S4 Expression of Fundc1 in different tissues and its response to hypoxia. (a) Fundc1 mRNA distribution pattern in different mouse tissues. The distribution of Fundc1 mRNA in different mouse tissues was determined by RT-PCR. Hprt as a loading control. (b) Fundc1 mRNA level in response to hypoxia in HeLa cells. Fundc1 mRNA level was determined by real-time PCR at 0, 6, 12, 24 h under hypoxic conditions. Data acquired from three independent experiments were normalized to the mRNA level of 0 h (mean ± s.e.m.), **p<0.01. NS, not significant. (c) Fundc1 protein expression level under hypoxic conditions in mouse brain. C57BL/6 mice are subjected to an atmosphere of 8% O_2 in nitrogen for 72 h and Western blotting was used to detect the protein levels of Fundc1 and other mitochondrial proteins.

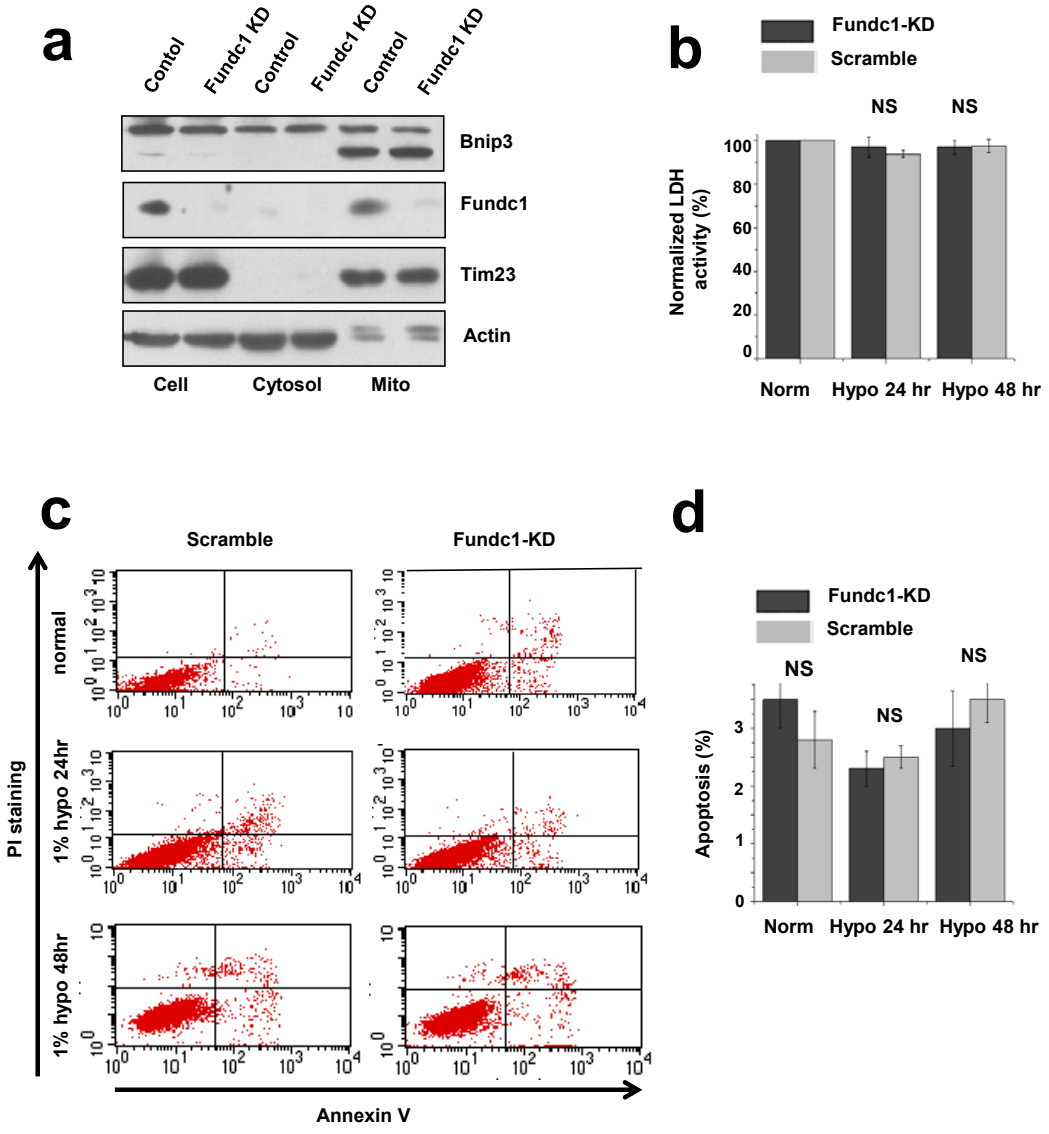

Figure S5 Knockdown of Fundc1 does not affect the expression and distribution of Bnip3 or cell viability under hypoxic conditions. (a) Control and Fundc1 KD HeLa cells were fractionated into cytosol and mitochondria, and analyzed for the distribution of Bnip3 by Western blotting. Fractionation quality was verified by the distribution of specific subcellular markers: Tim23 for mitochondria and actin for cytosol. (b) LDH release assay. Control and Fundc1 KD HeLa cells exposed to 1% O_2 for 0, 24 and 48 h. Media were then collected for measuring LDH activity. Data were normalized to the LDH activity of 0 h (mean ± s.e.m.; data were from three independent experiments). NS, not significant. (C) Control and Fundc1 KD HeLa cells were exposed to 1% O_2 for 0, 24 and 48 h, cells were stained with annexin V-FITC and propidium iodide (PI) and analyzed by flow cytometry. (D) Statistical graph of annexin V-FITC/PI staining. The percentage of apoptotic cells was calculated based on three independent experiments (mean ± s.e.m.). NS, not significant.

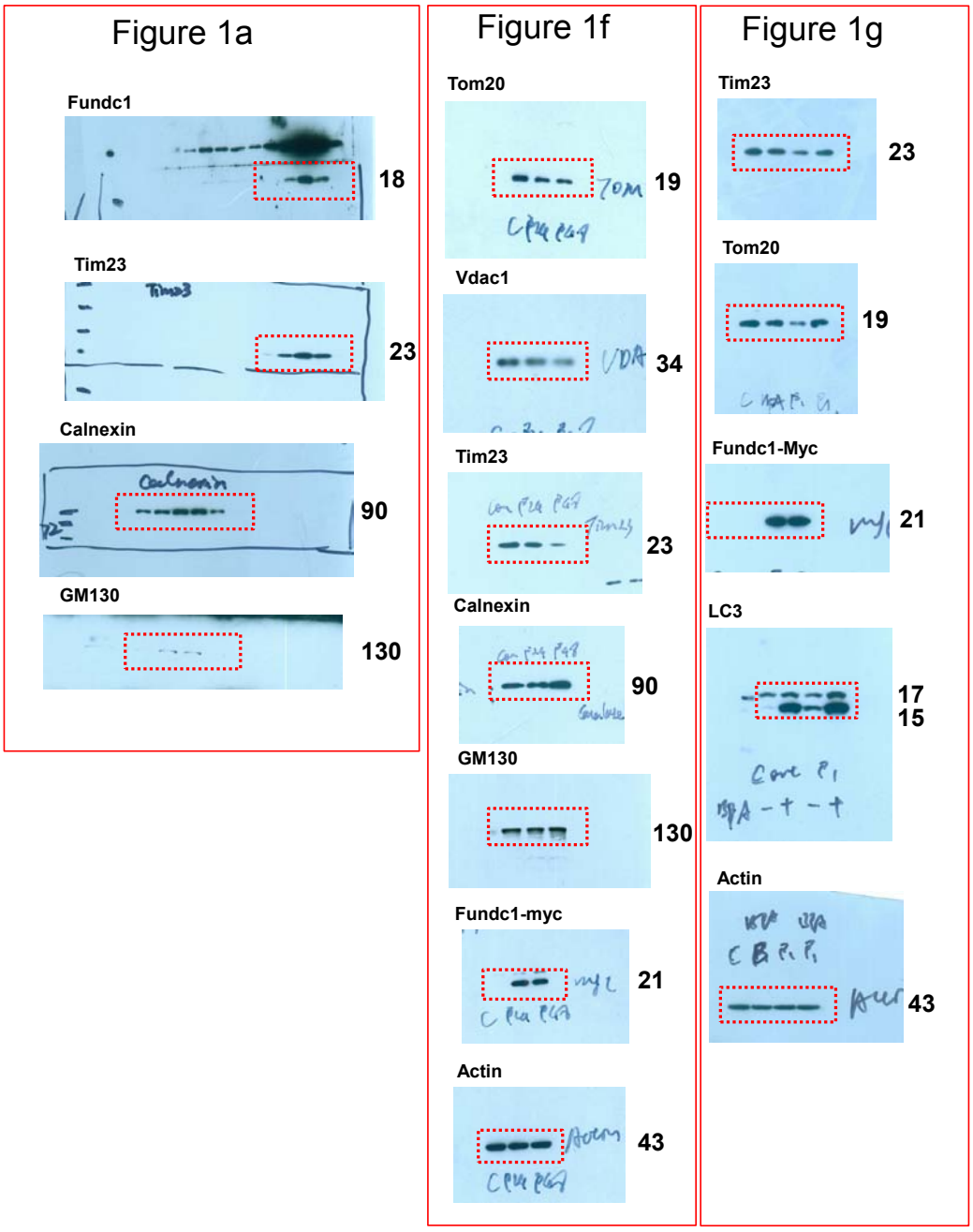

Figure S6 Full scans of original Western blots for data in figure 1, 2, 3, 4, 5. Panels corresponding to the figures in the paper are indicated.

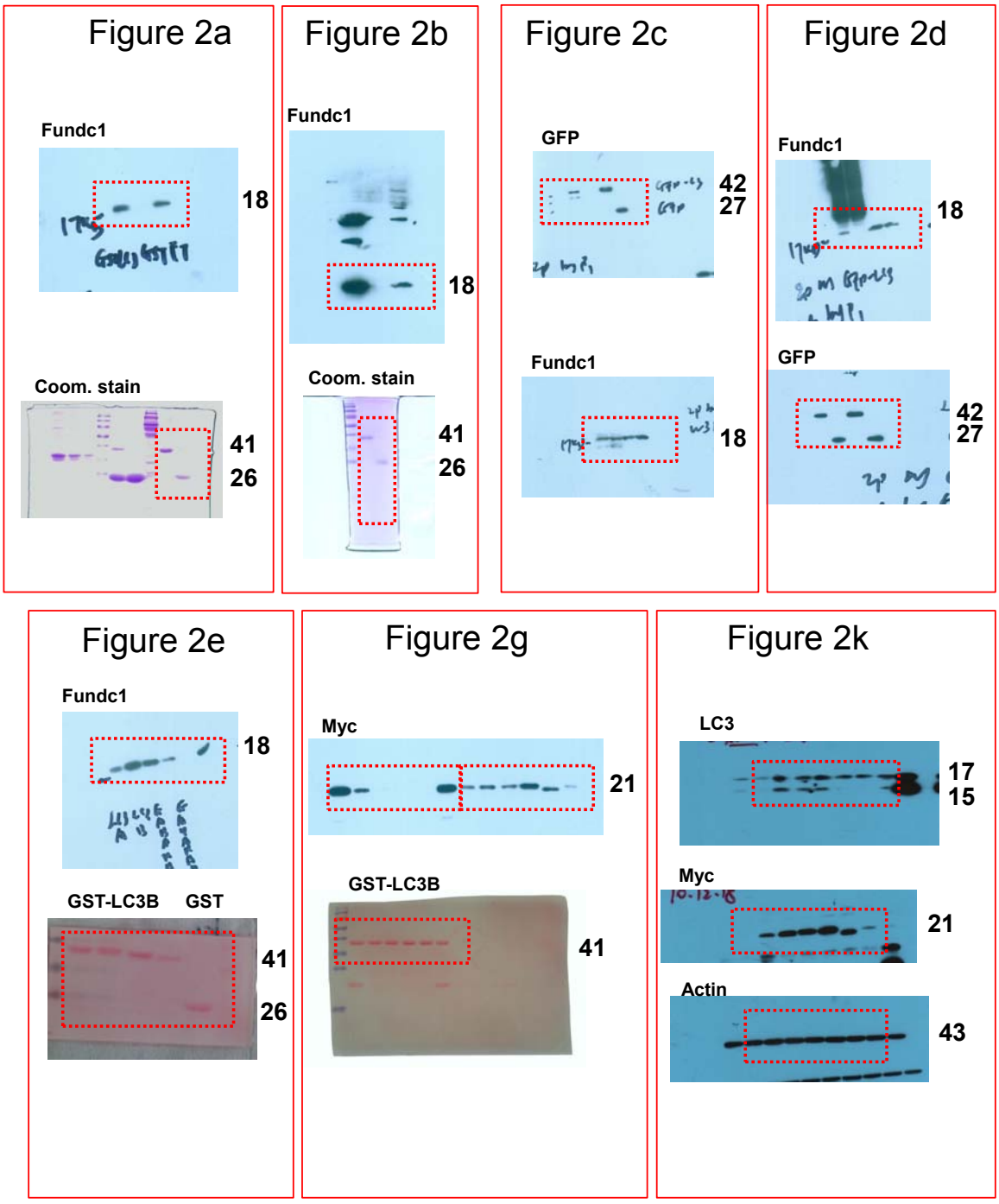

Figure S6 continued

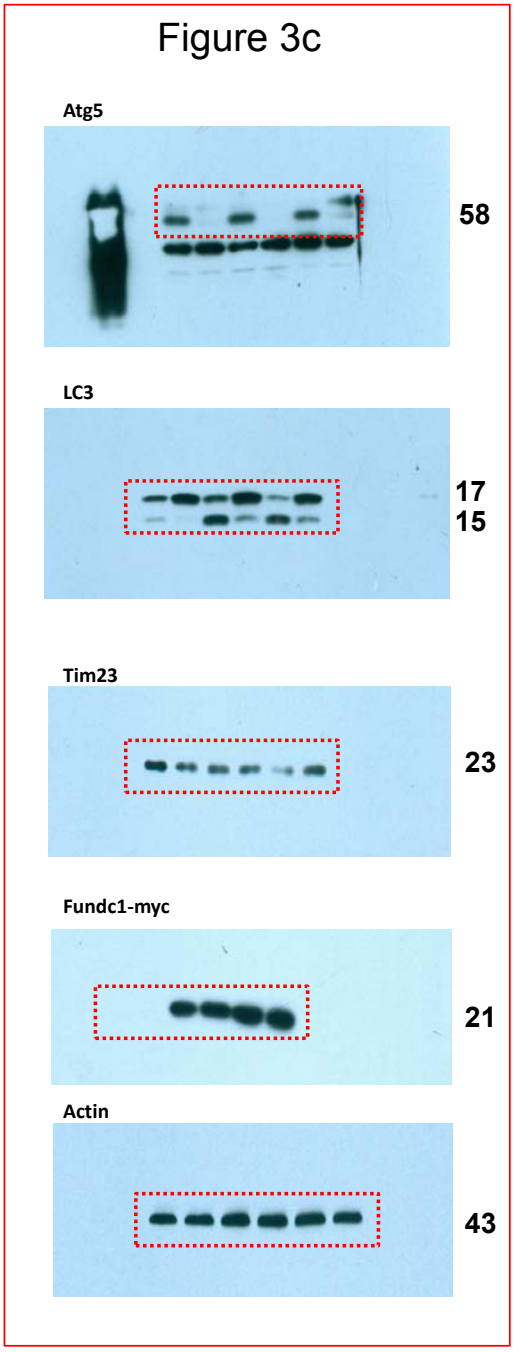

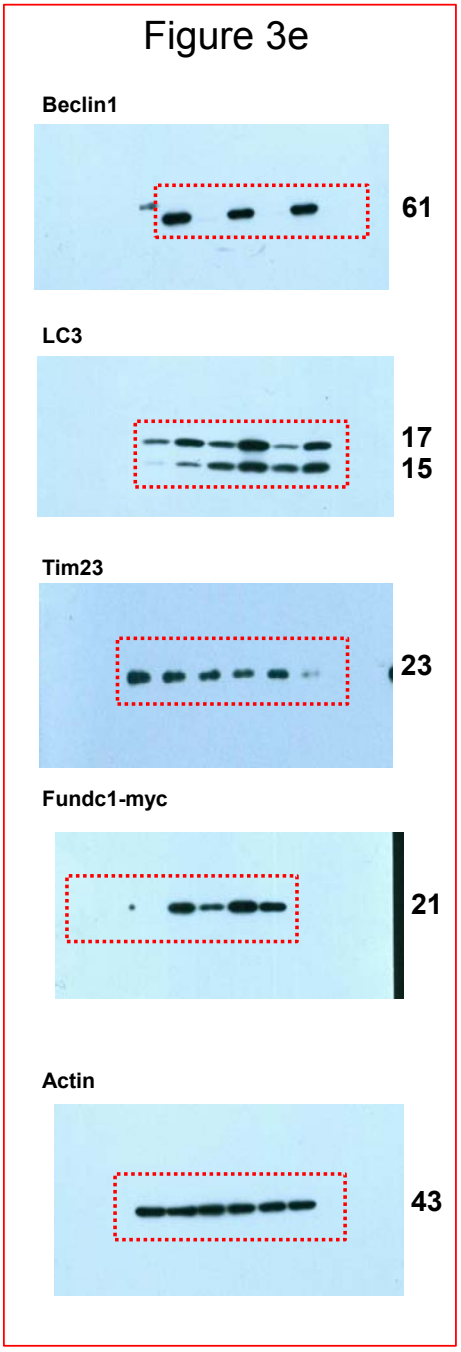

Figure S6 continued

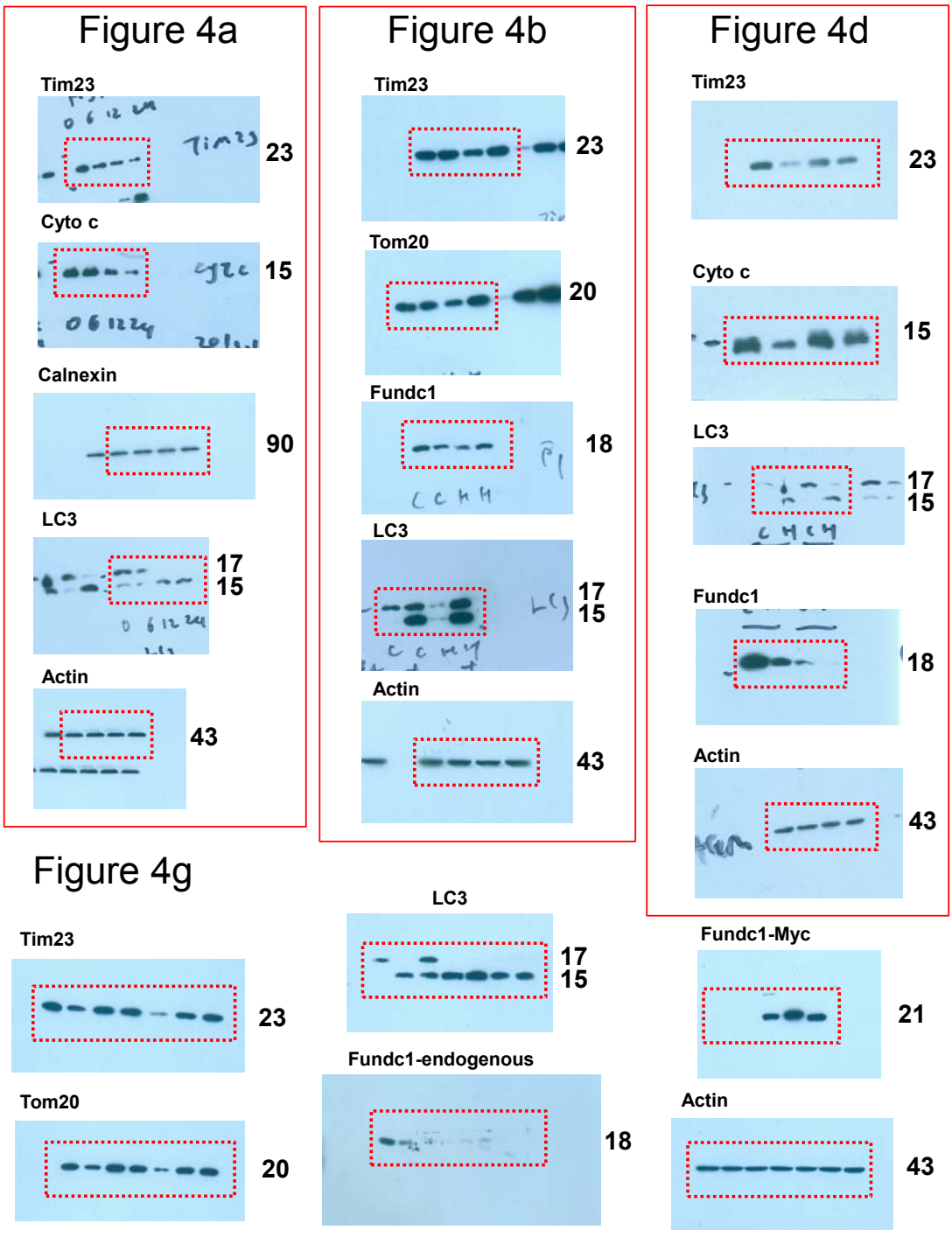

Figure S6 continued

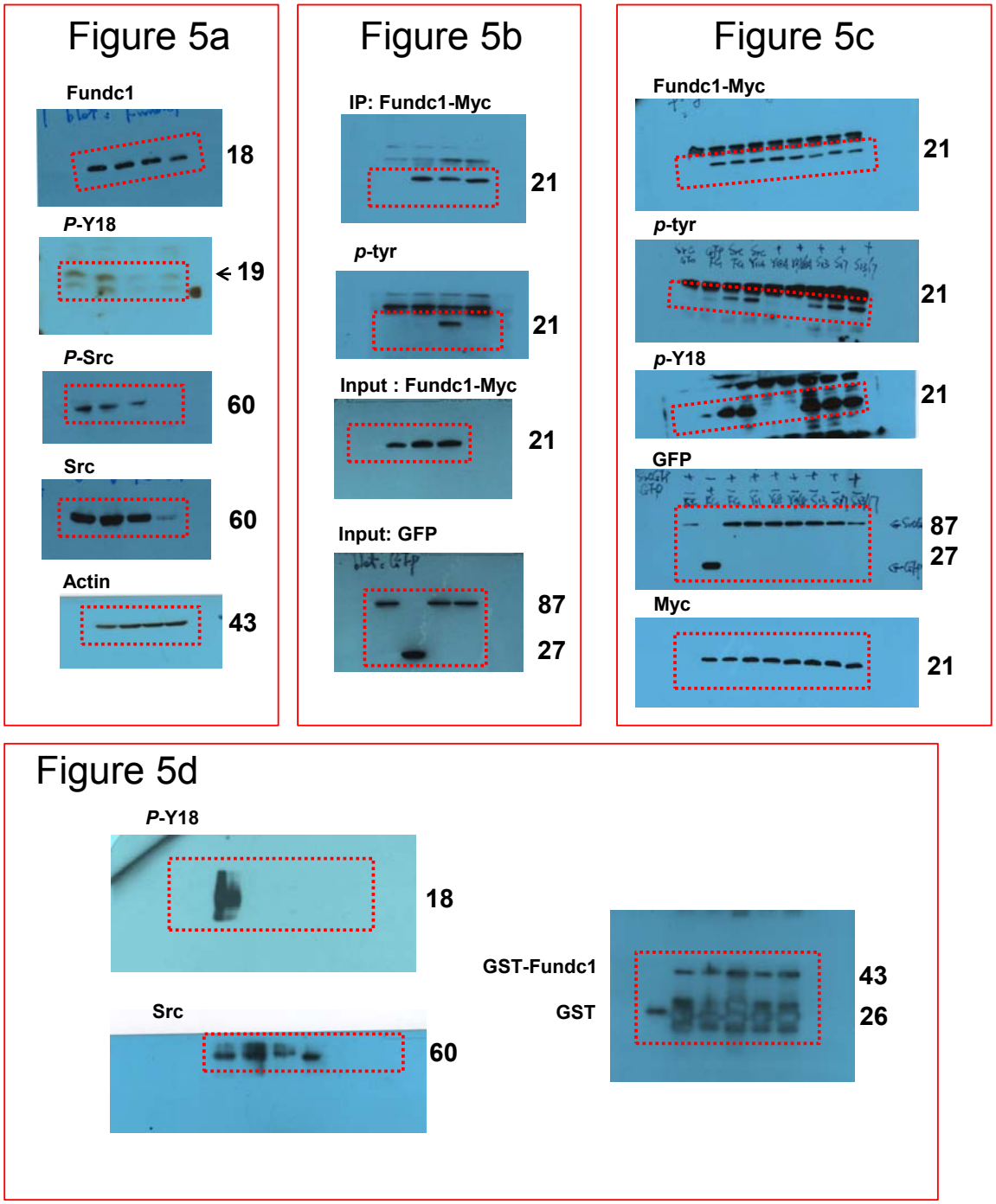

Figure S6 continued

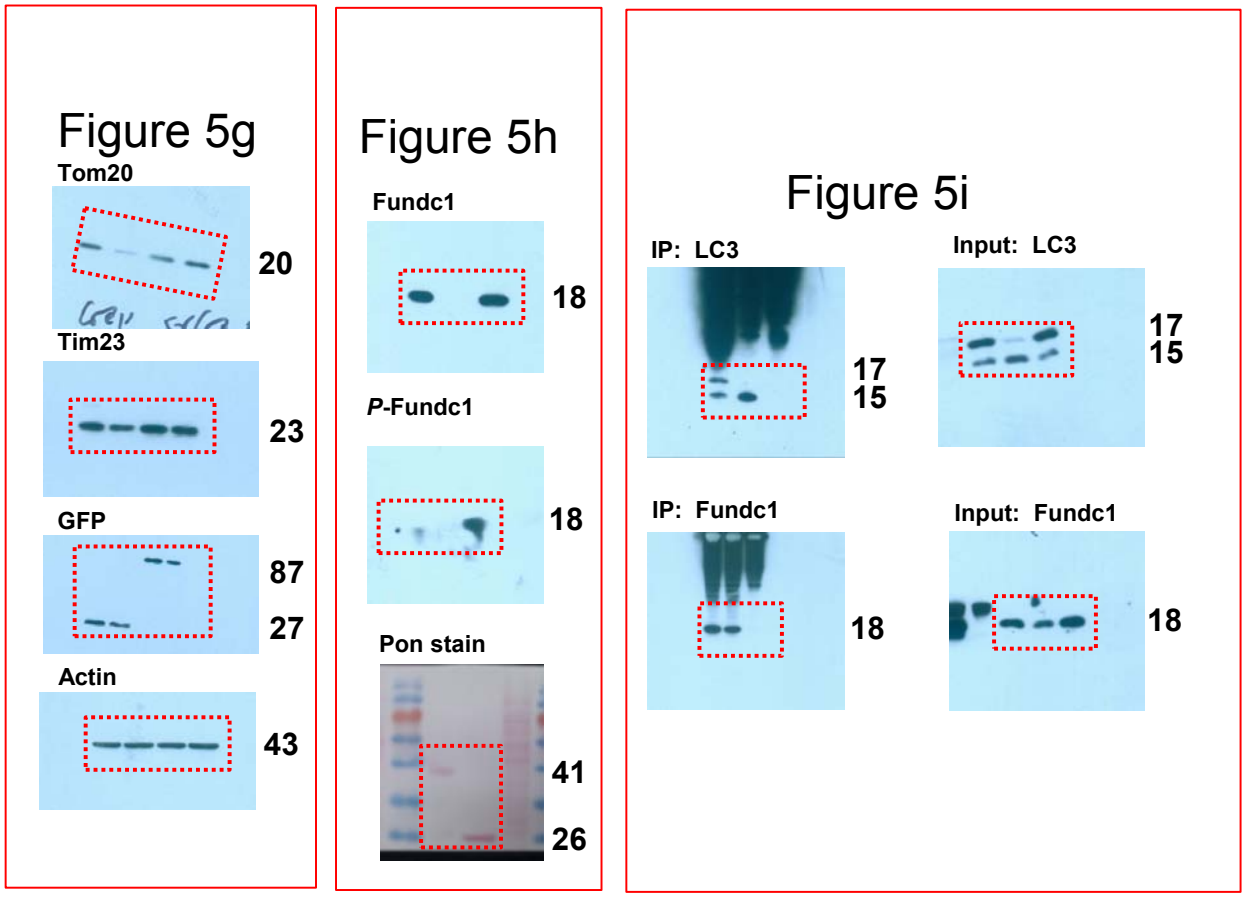

Figure S6 continued